2019

Solvation Properites of Supercritical Carbon Dioxide Using Chirped-Pulse Fourier-Transform Microwave Spectra of Carbon Dioxide / 1, 1-Difluoroethene (DFE) Mixtures

Tulana Ariyaratne Subasinghe Arachchige

Recommended Citation

The Graduate School
EASTERN ILLINOIS UNIVERSITY

Thesis Maintenance and Reproduction Certificate

FOR: Graduate Candidates Completing Theses in Partial Fulfillment of the Degree
         Graduate Faculty Advisors Directing the Theses

RE: Preservation, Reproduction, and Distribution of Thesis Research

Preserving, reproducing, and distributing thesis research is an important part of Booth Library's responsibilit to provide access to scholarship. In order to further this goal, Booth Library makes all graduate theses completed as part of a degree program at Eastern Illinois University available for personal study, research, and other not-for-profit educational purposes. Under 17 U.S.C. § 108, the library may reproduce and distribute a copy without infringing on copyright; however, professional courtesy dictates that permission be requested from the author before doing so.

Your signatures affirm the following:

• The graduate candidate is the author of this thesis.

• The graduate candidate retains the copyright and intellectual property rights associated with the original research, creative activity, and intellectual or artistic content of the thesis.

• The graduate candidate certifies her/his compliance with federal copyright law (Title 17 of the U. S. Code) and her/his right to authorize reproduction and distribution of all copyrighted materials included in this thesis.

• The graduate candidate in consultation with the faculty advisor grants Booth Library the nonexclusive, perpetual right to make copies of the thesis freely and publicly available without restriction, by means of any current or successive technology, including but not limited to photocopying, microfilm, digitization, or internet.

• The graduate candidate acknowledges that by depositing her/his thesis with Booth Library, her/his work is available for viewing by the public and may be borrowed through the library's circulation and interlibrary loan departments, or accessed electronically. The graduate candidate acknowledges this policy by indicating in the following manner:

_____Yes, I wish to make accessible this thesis for viewing by the public

___X___No, I wish to quarantine the thesis temporarily and have included the *Thesis Withholding Request Form*

• The graduate candidate waives the confidentiality provisions of the Family Educational Rights and Privacy Act (FERPA) (20 U. S. C. § 1232g; 34 CFR Part 99) with respect to the contents of the thesis and with respect to information concerning authorship of the thesis, including name and status as a student at Eastern Illinois University. I have conferred with my graduate faculty advisor. My signature below indicates that I have read and agree with the above statements, and hereby give my permission to allow Booth Library to reproduce and distribute my thesis. My adviser's signature indicates concurrence to reproduce and distribute the thesis.

Solvation properties of supercritical carbon dioxide using chirped-pulse Fourier-transform

microwave spectra of carbon dioxide / 1,1-difluoroethene (DFE) mixtures

(TITLE)

BY

Tulana Ariyaratne Subasinghe Arachchige

THESIS

SUBMITTED IN PARTIAL FULFILLMENT OF THE REQUIREMENTS
FOR THE DEGREE OF

Master of Science in Chemistry

IN THE GRADUATE SCHOOL, EASTERN ILLINOIS UNIVERSITY
CHARLESTON, ILLINOIS

2019

YEAR

I HEREBY RECOMMEND THAT THIS THESIS BE ACCEPTED AS FULFILLING
THIS PART OF THE GRADUATE DEGREE CITED ABOVE

Solvation properties of supercritical carbon dioxide (sc-CO$_2$) using chirped-pulse Fourier-transform microwave spectra of CO$_2$ / 1,1-difluoroethene (DFE) mixtures

Acknowledgments

Abstract

Supercritical carbon dioxide (sc-CO_2) is a highly utilized industrial substance identified as an excellent solvent and a surfactant, which is cheaper and less hazardous than other typical solvents. The higher solubility of fluorinated hydrocarbons than their hydrocarbon (HC) analogs is not well understood and the theory behind the microsolvation of sc-CO_2 cannot be fully explained with the existing chemical information. Microwave spectroscopy is a good method of identifying the structural arrangement of clusters made from fluorinated HCs and CO_2. In this project, microwave scans of the four different mixtures of 1,1-difluoroethene (DFE) and CO_2 were studied and additionally a pure DFE scan was studied additionally. A chirped-pulse Fourier-transform (FTMW) microwave spectrometer was used to obtain the scans. The DFE and CO_2 clusters can be easily identified using microwave spectroscopy because DFE is a very polar molecule and CO_2 has an induced dipole moment respectively. The relative intensities of the peaks in the scans and the rotational constants were considered to identify the molecular clusters. Previously identified DFE / CO_2 dimer structures were helpful to predict the bigger structures manually. Apart from that, the ABCluster application was used to predict the bigger structures, as guessing stable structures in three dimensions becomes harder as the cluster becomes bigger. All the predicted and approximated structures were optimized using Gaussian09W. One spectrum was identified in the DFE / CO_2 scans, and after comparing the intensities and rotational constants, it was confirmed as a DFE / $(CO_2)_3$ tetramer. In this structure, one CO_2 is located above the DFE plane, another CO_2 is located side of DFE and the other CO_2 is located top-above of the DFE. One spectrum was identified in pure DFE scan and it was confirmed as a $(DFE)_3$ trimer. In that

structure, two DFEs are facing each other invertedly and the third DFE is located above the first two DFEs. This study aims to identify the solvation shell CO_2 makes around DFE when it dissolves. Hence, the maximum number of CO_2 molecules binding to a DFE molecule needs to be identified. A parallel study is occurring with vinyl fluoride (VF) / CO_2 and these studies collectively provide information about the variation in the number of CO_2 molecules that bind as the number of fluorine atoms attached to the same HC analog is varied. In the future, MathCAD applications will be used to identify largely spaced fingerprint patterns to find other stable clusters present in the experiment. Also, ^{13}C isotopic studies will be done to confirm and compare the identified current structures.

Content

4. Discussion and conclusion

List of figures

List of tables

Chapter 1

1. Introduction

1.1 Supercritical CO_2 as a solvent and its importance

Any substance can be characterized as a supercritical fluid when that substance's temperature and the pressure is increased beyond its critical point. The supercritical fluid concept was brought up to the science world by the French physicist Charles Cagniard de La Tour in 1822.[1,2]

Supercritical carbon dioxide (sc-CO_2) and supercritical water (sc-H_2O) are highly utilized supercritical fluids in industry because of their excellent ability to act as a solvent and hence the ability to use that for extraction. sc-CO_2 can be observed when it is brought to its critical temperature (T_c) 31.1 °C and pressurized to its critical pressure (P_c) 72.8 bar.[3] Physically when CO_2 reaches its supercritical phase, its existing liquid-gas surface boundary disappears. sc-CO_2 acts as a better solvent than volatile organic compounds (VOC), because there is no surface tension like other volatile solvents (liquids); hence, when the pressure is reduced, the solute can be readily isolated. In that sense, having no surface tension like liquid is an extra advantage of sc-CO_2 in industrial applications.

sc-CO_2 is replacing current volatile organic compounds and it fits with the desired applications even better than previously used VOC. For example, decaffeination of coffee beans was done using dichloromethane (DCM) but now it is replaced by sc-CO_2 and H_2O. DCM is a carcinogenic substance, but there is no such danger with sc-CO_2 and H_2O.[4] Also, sc-CO_2 can be identified as a green chemistry substance because required CO_2 can be extracted from industrial CO_2 exhaust.[5] Although CO_2 is a greenhouse gas which is responsible for global warming, here, the CO_2 can be recycled several times.

sc-CO_2 dissolves fluorinated hydrocarbons (FHCs) better than hydrocarbons (HCs). This might be because fluorine is highly electronegative and it has a high electron affinity.[3] FHC has higher molecular volumes than its HC analogs which means that for, FHCs, the Hilde-brand solubility parameter (δ) (Equation 1.1) is significantly lower than its HC analog, where ΔH_V is enthalpy change through vaporization, R is gas constant, T absolute temperature and V_m is molar volume,[3] but this also does not provide a proper information for the reason behind the unexpected increasing soubilities of FHCs. For comparison, the solubilities of 2-fluoro-alpha-methyl-4-biphenylacetic acid ($C_{13}H_{13}FO_2$) and Naproxen ($C_{14}H_{14}O_3$) in sc-CO_2 have been compared, showing that the fluorinated compound's solubility in sc-CO_2 is ten times higher than the non-fluorinated compound.[6]

$$\delta = \sqrt{\frac{\Delta H_V - RT}{V_m}} \qquad (1.1)$$

Hence for this research 1,1-difluoroethene (DFE) has been used (Figure 1.1). Currently, this research group is studying fluorinated hydrocarbons and their solubility in sc-CO_2, because the reasons for fluorinated hydrocarbons being more CO_2-philic than hydrocarbon counterparts have not been fully explored.[7] The main theme of the research is studying the microsolvation of sc-CO_2 and the solvation shell it makes. It is important to study CO_2 attraction towards different fluorinated ethene molecules and the variation of number of CO_2 molecules arranged around the fluorinated ethene molecule when the number of fluorine atoms attached varies.

Microwave spectroscopy of a molecule or a cluster of the molecule is possible if the molecule or the molecular cluster has a net dipole moment; so it has to be a polar molecule. With 1,1-difluoroethene, there is no doubt that it has a dipole moment, but CO_2

3

is a nonpolar molecule, although it has been observed to have some polarity in CO_2 clusters because of the induced dipole moment.
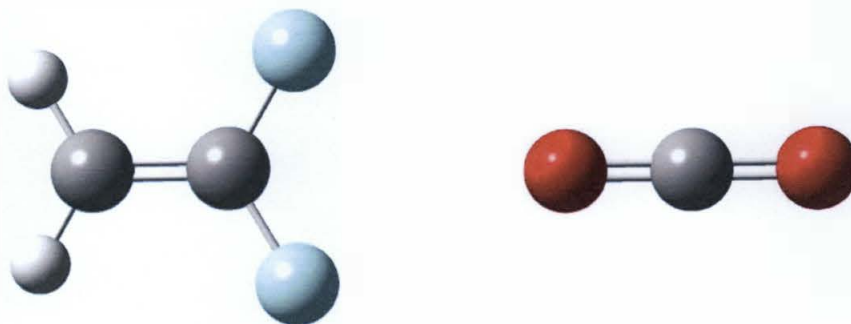
Figure 1.1 - 1,1-difluoroethene (left) and CO_2 (right)

1.2 Rotational spectroscopy

Rotational spectroscopy is also known as microwave spectroscopy because it uses microwaves to measure rotational transitions of molecules and molecule clusters in the gaseous phase. This is also known as pure rotational spectroscopy to distinguish this from rotational-vibrational spectroscopy where the energies are changed between rotational and vibrational energies. If there is no net dipole moment in a molecule or in a molecule cluster, the rotational spectrum cannot be observed. For nonpolar molecules, Raman spectroscopy and infrared spectroscopy (for many cases) can be used to observe their structural characteristics. As instead of rotational motion of a cluster, in infrared spectroscopy, it detects the molecular vibrations and in Raman spectroscopy, it detects the molecular deformation in an electric field determined by molecular polarizability α.
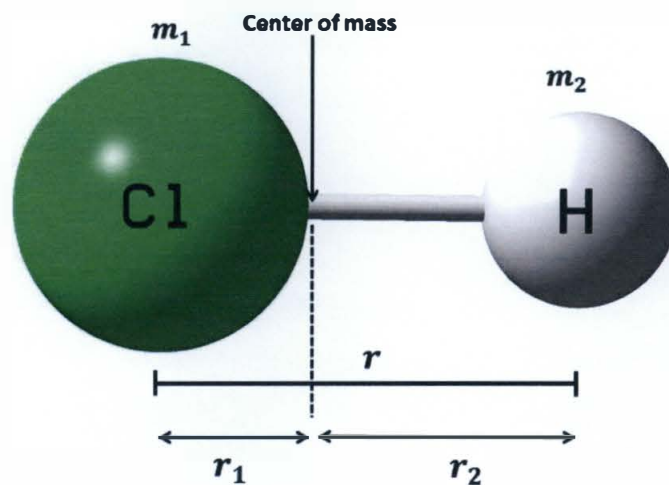
Figure 1.2 - Rotation of a rigid rotor

When a diatomic molecule is rotating as shown in Figure 1.2, the mass can be calculated as reduced mass (μ) and it can be obtained from (Equation 1.2),

$$\mu = \frac{m_1 m_2}{(m_1 + m_2)} \qquad (1.2)$$

For a diatomic molecule, the moment of inertia (I) or the reluctance to the rotation can be given from (Equation 1.3),

$$I = \mu r^2 \qquad (1.3)$$

Also the angular velocity of the motion is given as, $\omega = 2\pi v_{rot}$.

The angular momentum (L) can be defined as below (Equation 1.4),

$$L = I\omega \qquad (1.4)$$

For a single atom of m mass, the kinetic energy can be defined as $k = \frac{1}{2}mv^2$. Hence for a multi-atomic structure with n number of atoms, the kinetic energy T can be defined (Equation 1.5).

$$T = \frac{1}{2}\sum_{i=1}^{n} m_i v_i^2 \tag{1.5}$$

As HCl has two atoms with masses m_1 and m_2, the equation for T can be observed as mentioned in equation 1.6.

$$T = \frac{1}{2}(m_1 r_1^2 + m_2 r_2^2)\omega^2 = \frac{1}{2} I\omega^2 \tag{1.6}$$

That is the classical mechanics approach to a rigid rotor's rotation. In the quantum mechanical approach, a diatomic molecule is considered as a quantum mechanical rigid rotor and its energy can be obtained solving the Schrödinger equation. By solving the equation, the rotational energy (E_J) can be obtained from equation 1.7 – 1.10. The energy can be given in a few forms. In 1.7 equation the energy is given in *Joules*.

$$E_J = \frac{\hbar^2}{2I}J(J+1) \tag{1.7}$$

But, $B' = \hbar^2/2I$ (in *J*). Hence, E_J can be written as in Equation 1.8.

$$E_J = B'J(J+1) \tag{1.8}$$

Also, $\hbar = h/2\pi$; h is Planck's constant. Hence B' can be written as in equation 1.9.

$$B' = \frac{h^2}{8\pi^2 I} \quad (in\ J) \tag{1.9}$$

6

The energy of E_J can be observed in *Hertz* as well as mentioned in equation 1.10.

$$E_J = \frac{\hbar^2}{2I}J(J+1) = BJ(J+1)h \qquad (1.10)$$

$$B = \frac{h}{8\pi^2 I} \qquad (in\ Hz) \qquad (1.11)$$

Here, the rotational constant is given in either *Hertz* (*Hz*) (Equation 1.11) or *Joule* (*J*) (Equation 1.9) and the rotational constants indicates information about the structure and the mass distribution of the molecule.

J is called *rotational angular momentum quantum number* which could be a positive integer such as 0, 1, 2, 3,.........∞. Consider the energy transition among two consecutive quantum numbers; $\Delta J = \pm 1$ (Equation 1.12 – 1.14).

$$E_{(J+1)} = B'(J+1)(J+2) \qquad (1.12)$$

$$E_{(J)} = B'J(J+1) \qquad (1.13)$$

$$\Delta E = E_{(J+1)} - E_{(J)} = B'(J+1)(J+2) - B'J(J+1) = 2B'(J+1) \qquad (1.14)$$

$$J+1 \qquad\qquad E_{(J+1)} = B'(J+1)(J+2)$$

$$\Delta E = E_{(J+1)} - E_{(J)} = 2B'(J+1)$$

$$J \qquad\qquad E_{(J)} = B'J(J+1)$$
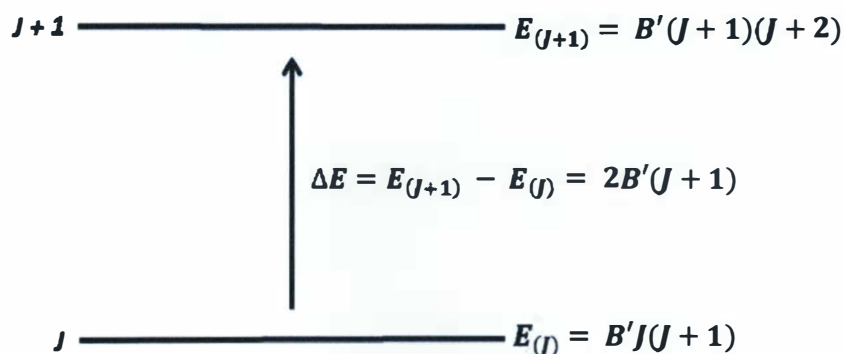
Figure 1.3 - The energy difference between two adjacent energy levels

The energy difference of the adjacent rotational energy levels increases by the multiples of $2B$ (Figure 1.3 and 1.4). For example when, $J_{1\leftarrow0}, \Delta E = 2B$, and when $J_{2\leftarrow1}, \Delta E = 4B$ and when $J_{3\leftarrow2}, \Delta E = 6B$, etc.
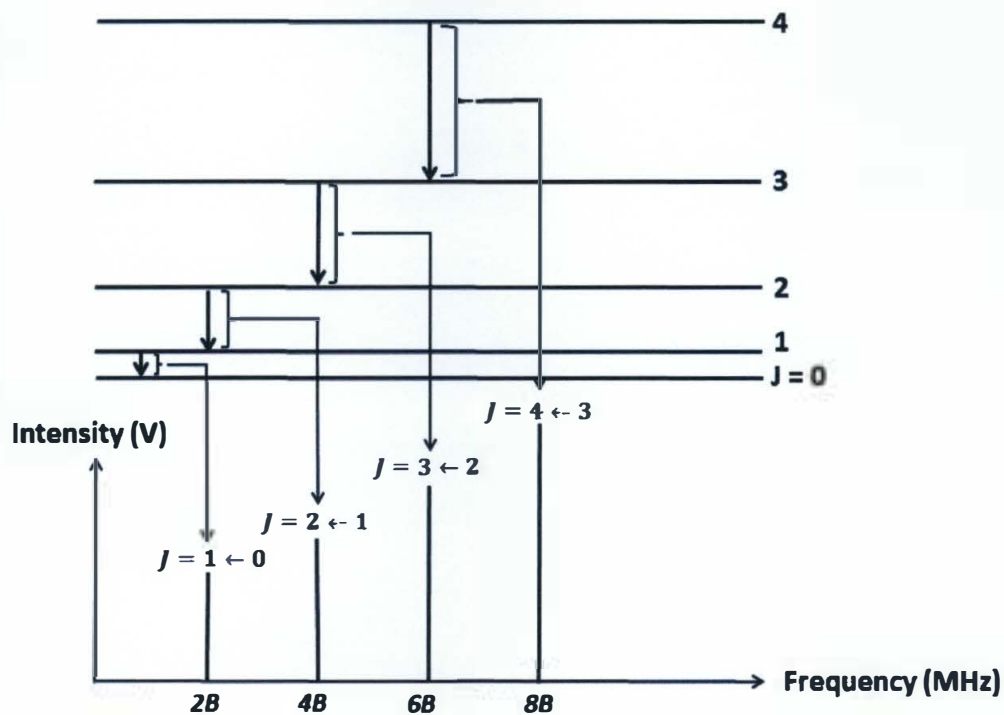
Figure 1.4 - The frequencies of the transitions and the related quantum numbers[8]

Taking the CH₃Cl molecule, more as an example which is three dimensional (Figure 1.5), the rotation is not limited to one direction but to three basic directions around its center of mass. The three axes a, b, and c are introduced to understand the three basic rotations. The a-axis is responsible for the highest rotational constant B_A, and then B_B and B_C (Figure 1.5). In practice, the rotational constants B_A, B_B, and B_C are named as A, B, and C respectively. The rotational constant has an inversely proportional relationship with its moment of inertia (I), and I is directly proportional to reduced mass.

8

Therefore around the a-axis where it has the highest rotational constant (A), the moment of inertia, I_a is at a minimum,
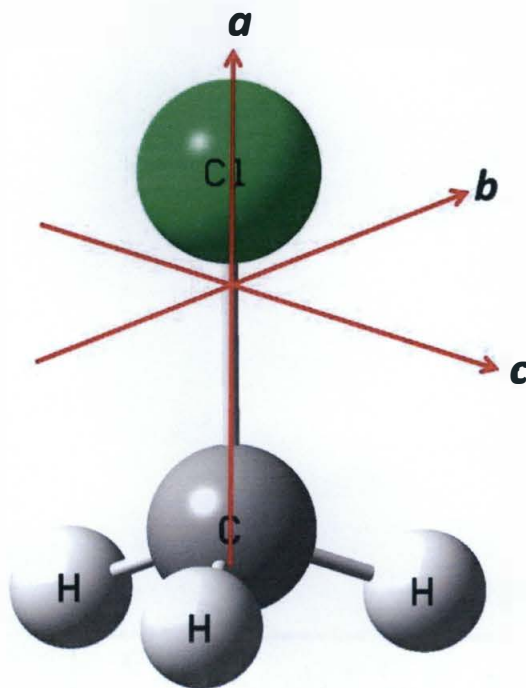
Figure 1.5 - Three rotational axes of CH₃Cl molecule

It is common that the rigid rotor approximation is not compatible with the experimental situations. Mostly it was observed that the experimental data did not tally with the theoretical data if the rigid rotor approximation is implemented. In fact, when the molecules are rotating faster with higher J values, the high centrifugal forces elongates the bonds away from the center of mass. Because of this stretching, molecules do not behave as a rigid rotor. The distortion constants (D) are introduced to make these theoretical values fit the experimental values, (Equation 1.15).

$$E_J = B\,J(J+1) - D\,J^2(J+1)^2 \qquad (1.15)$$
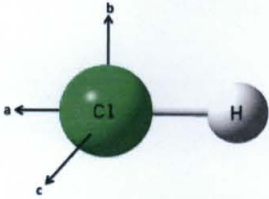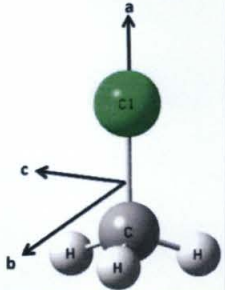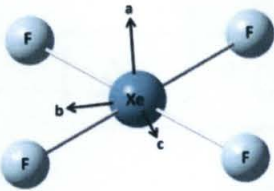
Where D, is equal to (Equation 1.16),

$$D = \frac{4B^3}{\omega^2} \qquad (1.16)$$

When describing the rotation of a non-linear molecule, the J quantum number is not enough to describe its rotation, because such a molecule has the freedom to rotate along three rotational axes. Due to the variation of three moment of inertia components, I_a, I_b, and I_c, the molecules can be categorized into main four categories (Table 1.1). Therefore, additionally, K_a and K_c quantum numbers have been introduced, which describe the angular momentum projections along the a and c axes respectively. The K_a and K_c quantum numbers are introduced because in this study, asymmetric top molecules are studied and it needs both K_a and K_c quantum numbers.

For example, $J = 2$, the asymmetric top molecule has five corresponding energy levels (Figure 1.6). In the middle of each line, when combining the two numbers at the end of the line, the quantum numbers of the corresponding energy level can be found. The quantum numbers are defined as $J_{Ka,Kc}$. So for an example, in Figure 1.6, as the $J = 2$, when $K_a = 1$ and $K_c = 2$, the complete quantum number can be described as 2_{12}.

Table 1.1 - Types of molecules according to the moment of inertia

Group		Moment of inertia and required quantum numbers
Linear		$I_a = 0$, $I_b = I_c$ Need only J
Symmetric tops	Prolate	$I_a < I_b = I_c$ Need J and K_a
	Oblate	$I_a = I_b < I_c$ Need J and K_c
Spherical tops		$I_a = I_b = I_c$ Need only J
Asymmetric tops		$I_a < I_b < I_c$ Need J, K_a, and K_c
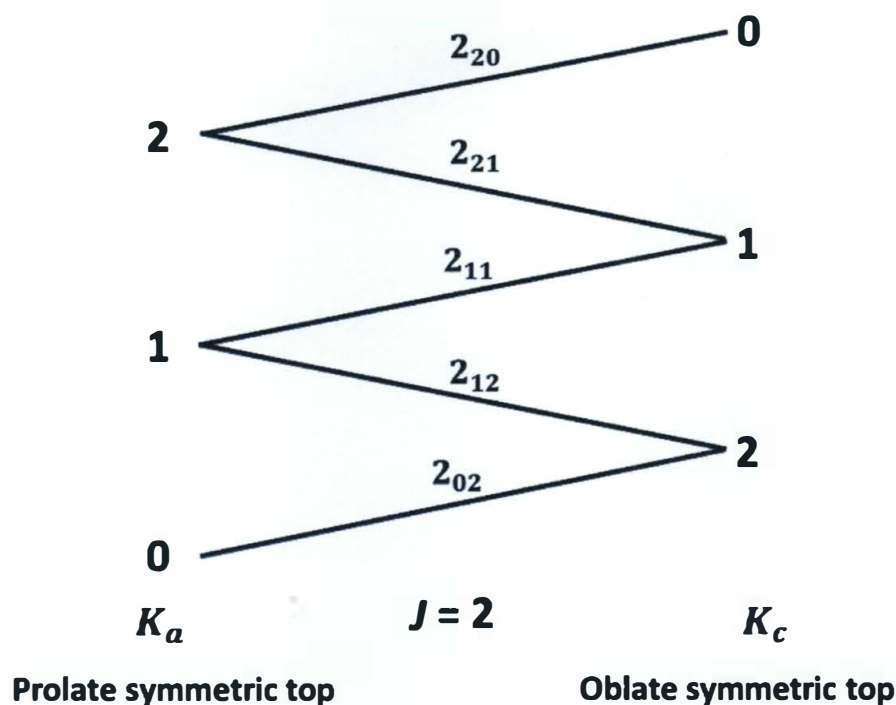
Figure 1.6 - Correlation diagram for $J = 2$ rotational energy levels. The two margins of the energy level diagram relate to prolate symmetric top (left) and oblate symmetric top (right). The asymmetric top molecule lies in-between prolate and oblate top molecules. Hence to describe an asymmetric top molecule's rotation, quantum number J, K_a and K_c are required [9]

In this study, for both projects, more than one distortion constant was used to make the data compatible with the experimental values. The energy expression can be expressed as below for a prolate symmetric rotor (Equation 1.17).[10]

$$E_{J,K} = BJ(J+1) + (A - B)K_a^2 - D_J J^2(J+1)^2 - D_{JK}J(J+1)K_a^2 + D_K K_a^4 \quad (1.17)$$

In equation 1.17, it can be seen that D_J, D_{JK}, and D_K are the only three distortion constants. But in this study, up to five distortion constants have been used including δ_J and δ_K, additionally. Equation 1.17 is not the full energy expression and when higher J quantum numbers are used, more distortion constants need to be introduced and consequently the energy expression is expanded.

Ray's asymmetry parameter (κ) is to measure the degree to which a molecule or a cluster is prolate or oblate. Prolate tops and oblate tops belong to the symmetric top category. Being an asymmetric top means that it has no rotational constants that are equal to one another ($I_a \neq I_b \neq I_c$), but many asymmetric top molecules are close to one of the symmetric top limits. The shape of the symmetric top structures can be seen from Table 1.1. From equation 1.18, κ can be obtained and for a prolate top it equals to $\kappa = -1$ and for an oblate top, it equals to $\kappa = +1$, so for any asymmetric top molecule, this κ value varies in between +1 and -1.

$$\kappa = \frac{2B-A-C}{A-C} \qquad (1.18)$$

Planar moment (P_{xx}) helps with structure determination. For three axes, P_{aa}, P_{bb} and P_{cc} can be defined (Equation 1.19 – 1.21). These three parameters are useful when determining the structure and the mass distribution along the a, b, and c axes. For example in DFE / CO_2 dimer study, for the first DFE / CO_2 structure (I) (Figure 1.7), P_{cc} is close to zero and that means along the c axis, there is no mass distributed and it is a planar structure.[11] Sometimes even for planar structures, P_{cc} can be not exactly equal to zero because of the vibrational effect in the molecules. As the distance provides the average distance where the atoms locate and those atoms are not always lie in the expected plane so the P_{cc} is not exactly zero.

$$P_{aa} = \sum_i m_i a_i^2 = 0.5(I_b + I_c - I_a) \qquad (1.19)$$

$$P_{bb} = \sum_i m_i b_i^2 = 0.5(I_a + I_c - I_b) \qquad (1.20)$$

$$P_{cc} = \sum_i m_i c_i^2 = 0.5(I_a + I_b - I_c) \qquad (1.21)$$

13
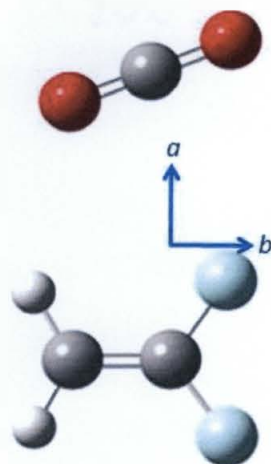
Figure 1.7 - DFE / CO$_2$ dimer structure (I) with P_{aa} = 449.86950(31), P_{bb} = 88.10054(31) and P_{cc} = 0.61469(31) [11]

As there exist three axes, *a, b* and *c*, there are three dipole moment components, μ_a, μ_b, and μ_c, respectively. According to the variation of these values, the structures again can be categorized into three types according to the freedom of quantum number changes. The selection rules are described in Table 1.2.

Table 1.2 - Selection rules for *a*-type, *b*-type and *c*-type transitions

Type of transition	Dipole moment	ΔJ	ΔK_a	ΔK_c
a-type	$\mu_a \neq 0$	0, ±1	0	±1
b-type	$\mu_b \neq 0$	0, ±1	±1	±1
c-type	$\mu_c \neq 0$	0, ±1	±1	0

1.3 Instrumentation and optimization

This thesis has two main projects in it. The first one is the analysis of spectra of DFE (1,1-difluoroethene) and CO$_2$ mixtures and the next project is the analysis of the spectrum of pure DFE sample. For DFE / CO$_2$ mixtures, 1% DFE is mixed with 1%, 2%, 3% and 4% of CO$_2$ at a time. The sample was mixed with 2 atm Ne as a carrier gas, and the spectrum was obtained from 2 GHz to 8 GHz using the chirped-pulse Fourier-

transform microwave (FTMW) spectrometer at the University of Virginia (UVa). The gas mixtures/sample were injected to the microwave vacuum chamber through five 1 mm nozzles at three times per second.

The theoretical structure identification for DFE / CO_2 spectrum was done using the existing information from the identified DFE / CO_2 dimer structures[11] and also using the ABCluster application.[12,13] ABCluster does a basic structure identification using Coulomb-Lennard-Jones potential. *Ab initio* calculations were done using Gaussian09W[14] at ωB97X-D/6-31+G(d,p) level to optimize the theoretical structures which have been obtained from the manual method (see below) or from ABCluster.

The manual method refers to arranging the bigger molecular clusters to optimize, and that arrangement was done by getting the information from the previous studies of DFE / CO_2.[11] In search of bigger clusters which contain DFE / CO_2, its dimer structure was used to deduce the bigger cluster. In the previous studies, the existence of four stable structures of DFE / CO_2 dimers have been found theoretically. In this manual method, the goal is to arrange the trimer, tetramer and pentamers of DFE / CO_2 the way it is arranged in the four dimer structures. The other method is deducing the structure using ABCluster. It is an application which uses artificial intelligence (AI) to find the lowest energy stable clusters among a pool of possible arrangements. Though it does not give very accurate and precise information, the level of accuracy it provides is enough as all the information can be directly fed to *ab initio* optimization. Both of these methods are discussed in detail in Chapter 2. "Experimental Analysis of DFE / CO_2 spectra".

1.4 Previous studies on other DFE / CO_2 structures

This project is about DFE / CO_2 mixtures and the spectrum for a pure DFE sample. Pure DFE studies have not been done previously, so there information about the structural arrangement is very limited. Due to this, all the initial structural analysis was done using ABCluster. For DFE / CO_2 a lot of literature information is available and most of the data were taken from the DFE / CO_2 dimer study.[11] In that study, four stable theoretical dimer structures were identified and out of those four, one was found experimentally in the spectrum. As it was previously mentioned, the main goal of this study is to identify the solvation shell that CO_2 forms when it dissolves fluorinated hydrocarbons (FHCs). The reason for fluorinated HCs being more CO_2-philic than their equivalent HC is another unresolved problem which existing information in chemistry cannot explain well. Understanding this better is another goal of this study. So collectively studying different types of fluorinated HCs would help to understand the maximum number of CO_2 molecule that can be attracted to a fluorinated hydrocarbon (FHC) when the number of F atoms is changing.

For that, different fluorinated HC mixtures with CO_2 need to be used, and currently, that is being done by this research group. At the moment 1,1-difluoroethene and vinyl fluoride are being used as the fluorinated HCs. The maximum number of CO_2 molecules that can bind to fluorinated HCs still has not been confirmed, but with the previous study information, the solvation shell of the system is slowly being revealed while finding bigger clusters with more CO_2 molecules attached to the fluorinated HCs.

References

[1] Anonymous. Explore, use, make the most of supercritical fluids. Le Portail des fluides supercritiques. http://www.supercriticalfluid.org/Supercritical-fluids.146.0.html [04/09/2019]

[2] Anonymous. Cagniard de la Tour, Charles. https://en.wikisource.org/wiki/1911_Encyclop%C3%A6dia_Britannica/Cagniard_de_la_Tour,_Charles [04/09/2019]

[3] Peach, J.; Eastoe. J. Supercritical carbon dioxide: a solvent like no other. *Beilstein J. Org. Chem.* **2014**, *10*, 1878.

[4] Anonymous. Dichloromethane. SIGMA-ALDRICH. https://www.sigmaaldrich.com/chemistry/solvents/dichloromethane-center.html [04/11/2019]

[5] Anastas, P. T.; Warner, J. C. Green Chemistry: Theory and Practice; Oxford University Press: New York, **1998**.

[6] Abdullah, S. A. Solubility in supercritical carbon dioxide. Department of chemical engineering. New Jersey Institute of Science and Technology, Newark. NJ. **2007**.

[7] Kannangara, P. B.; West, C. T.; Peebles, S. A.; Peebles, R. A. Towards microsolvation of fluorocarbons by CO_2: Two isomers of fluoroethylene-$(CO_2)_2$ observed using chirped-pulse Fourier-transform microwave spectroscopy. *Chem. Phys. Lett.* **2018**, *706*, 538.

[8] Anonymous. Chemistry LibreText. https://chem.libretexts.org/Bookshelves/Physical_and_Theoretical_Chemistry_Textbook_Maps/Supplemental_Module s_(Physical_and_Theoretical_Chemistry)/Spectroscopy/Rotational_Spectroscopy/Microwave_Rotational_Spectroscopy [05/02/2019]

[9] Townes, C. H.; Schawlow, A. L. Microwave Spectroscopy. Dover Publications Inc. **1975**, 86.

[10] Hollas, J. M. Modern spectroscopy. Fourth edition. John Wiley & Sons, Ltd. **2004**, 114.

[11] Anderton, A. M.; Peebles, R. A.; Peebles, S. A. Rotational Spectrum and Structure of the 1,1-Difluoro-ethylene···Carbon Dioxide Complex. *J. Phys. Chem. A* **2016**, *120*, 247.

[12] Zhang, J.; Dolg, M. ABCluster: The Artificial Bee Colony Algorithm for Cluster Global Optimization. *Phys. Chem. Chem. Phys.* **2015**, *17*, 24173.

[13] Zhang, J.; Dolg, M. Global optimization of clusters of rigid molecules using the artificial bee colony algorithm. *Phys. Chem. Chem. Phys.* **2016**, *18*, 3003.

[14] Frisch, M. J.; Trucks, G. W.; Schlegel, H. B.; Scuseria, G. E.; Robb, M. A. Cheeseman, J. R.; Scalmani, G.; Barone, V.; Mennucci, B.; Petersson, G. A.; Nakatsuji, H.; Caricato, M.; Li, X.; Hratchian, H. P.; Izmaylov, A. F.; Bloino, J.; Zheng, G.; Sonnenberg, J. L.; Hada, M.; Ehara, M.; Toyota, K.; Fukuda, R.; Hasegawa, J.; Ishida, M.; Nakajima, T.; Honda, Y.; Kitao, O.; Nakai, H.; Vreven, T.; Montgomery, Jr., J. A.; Peralta, J. E.; Ogliaro, F.; Bearpark, M.; Heyd, J. J.; Brothers, E.; Kudin, K. N.; Staroverov, V. N.; Keith, T.; Kobayashi, R.; Normand, J.; Raghavachari, K.; Rendell, A.; Burant, J. C.; Iyengar, S. S.; Tomasi, J.; Cossi, M.; Rega, N.; Millam, J. M.; Klene, M.; Knox, J. E.; Cross, J. B.; Bakken, V.; Adamo, C.; Jaramillo, J.; Gomperts, R.; Stratmann, R. E.; Yazyev, O.; Austin, A. J.; Cammi, R.; Pomelli, C.; Ochterski, J. W.; Martin, R. L.; Morokuma, K.; Zakrzewski, V. G.; Voth, G. A.; Salvador, P.; Dannenberg, J. J.; Dapprich, S.; Daniels, A. D.; Farkas, O.; Foresman, J. B.; Ortiz, J. V.; Cioslowski, J.; Fox, D. J. Gaussian 09W, Revision E.01, Gaussian, Inc., Wallingford CT, **2013**.

Chapter 2

2. Experimental analysis of CO_2 / 1,1-difluoroethene (DFE) spectra

2.1 Introduction

This project is about identifying the solvation properties of supercritical CO_2 (sc-CO_2). When CO_2 is dissolving a solute (here it is DFE), CO_2 makes a solvation shell around the solute. It is desirable to identify the solvation shell that CO_2 makes around the molecule it dissolves and chirped-pulse Fourier-transform microwave spectroscopy is a suitable technique to study this. Increasing the number of CO_2 molecules and using different types of fluorinated hydrocarbons provides more information about the microsolvation ability of CO_2, which leads to developing a better model for microsolvation by sc-CO_2. The fact that fluorinated hydrocarbons have better solubility in CO_2 than the equivalent hydrocarbons,[1] leads to their industrial application as surfactants and dry cleaning agents. But the reasons behind their observation are not well explained. As discussed in the Introduction (Chapter 1.1), identification of sc-CO_2 solvation properties using microwave spectroscopy has a long history. In 1995 Bemish *et al* reported structural arrangements for the 1 ethylene (C_2H_4) / 1 CO_2 dimer.[2] Then in 2014 Christenholz *et al* replaced one H with F (vinyl fluoride, VF), so VF / CO_2 dimer structural arrangements were identified.[3] More recently, in 2016 Anderton *et al* studied 1,1-difluoroethene (DFE) with 1 CO_2.[4] The present project is an extension of the DFE / CO_2 dimer. At this time, the aim of the project is looking for bigger structures (trimer, tetramer, pentamer, etc.) containing DFE and CO_2 molecules.

2.2 Spectral analysis (Experimental)

For the experiment, chirped-pulse Fourier-transform microwave (CP-FTMW) spectra of DFE / CO_2 were collected with 1% DFE and four different CO_2

concentrations (1%, 2%, 3% and 4% CO_2), as was described in Chapter 1.3, 'Instrumentation and optimization' part.

The University of Virginia (UVa) CP-FTMW spectrometer provided averages of 400,000 individual spectra for each mixture across the $2 - 8$ GHz range.[5] While the CP-FTMW spectrometer at Eastern Illinois University is more sensitive for acquiring data than UVa spectrometer, the data collection time is very high using the EIU CP-FTMW for the same number of shots. So it is preferable to use the UVa spectrometer for broader spectral analysis, where the high number of averages is important. Some peaks were unique to one scan while other peaks appeared on all four scans. Figure 2.1, shows the same peak appearing in all four scans. The four obtained DFE / CO_2 spectra were displayed on the same graph using Origin (Figure 2.1).[6] Previous studies done on VF / CO_2, showed that when a dimer was compared with a trimer, the trimer intensity was $\sim$ 1% - 10% of the dimer intensity.[3,7] This information led to misidentifying the spectrum identity as a trimer. The intensity variation of the dimer (DFE / CO_2) to the identified spectrum ($\sim$ 10%) gave the indication that this spectrum is a result of the rotation of a bigger cluster than a dimer (could be a trimer or might be a tetramer). As it was expected, a unique peak pattern, named as a constant difference pattern (where the distance between the 1st and 2nd peaks and the 3rd and 4th peaks is the same) was identified in all four spectra (Figure 2.2), with the maximum intensity recorded in the 2% CO_2 / 1% DFE spectrum. The constant difference pattern is a term used to identify a unique pattern like in Figure 2.2, where peaks are separated by equal distances (d1 $\sim$ d2, with a 4.0 kHz uncertainty). Though the transitions are different, the energy difference between the two transitions is equal to each other (d1 $\sim$ d2) (Figure 2.3). The uncertainty of 4.0 kHz is determined by the quality of the spectrometer used. This spectrometer provides one data point (in V)

each and every 12.5 kHz (from 2 GHz to 8 GHz) and the average of such 400,000 points determines the final scan. It has been found that the University of Virginia spectrometer has a 4.0 kHz uncertainty. Before FTMW technology, the uncertainty associated with spectrometers (Stark modulation microwave spectrometer) used to be around 100 kHz.[8]
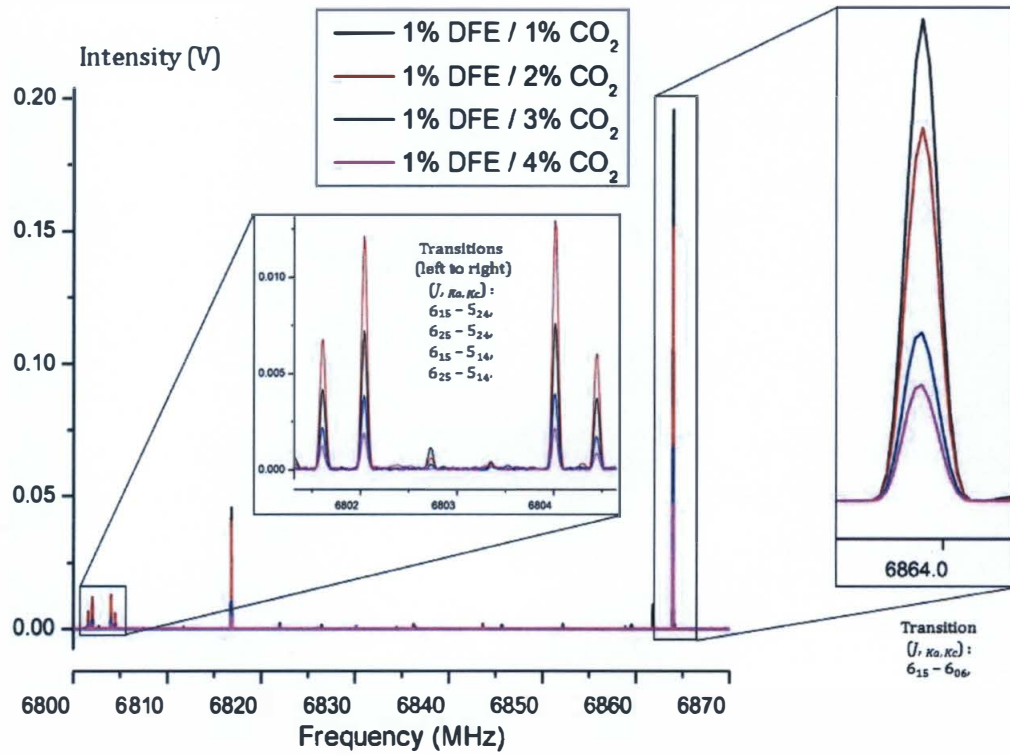
Figure 2.1 - Intensity variation of different species in four spectra with different CO_2 proportions. The DFE / CO_2 dimer is responsible for the peak around 6864 MHz (right) and the species identified recently in this project can be seen around 6803 MHz (left)
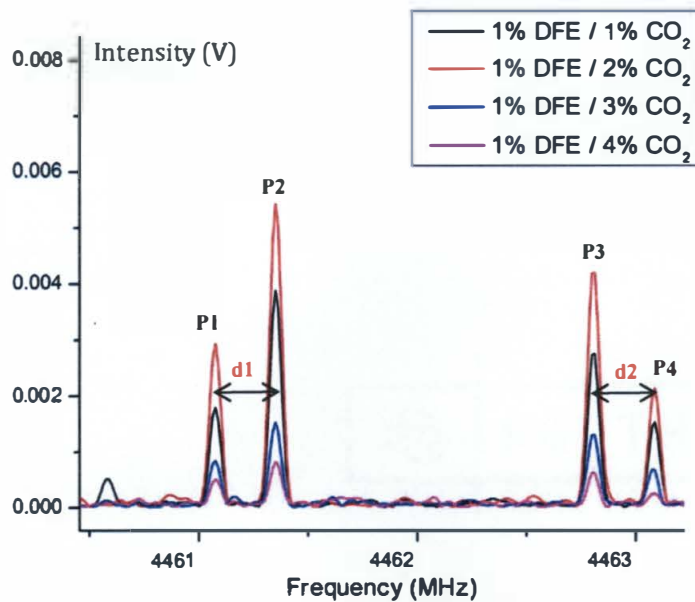
Figure 2.2 – A constant difference pattern in Origin. All scans give the peaks at the same frequency, which provides information about the same molecular cluster in the scans.
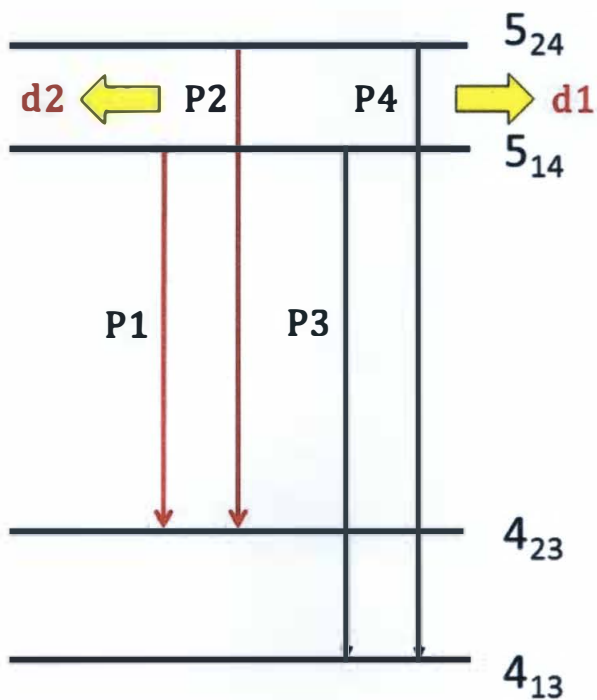
Figure 2.3 - The energy difference between d1 and d2. d1 ~ d2 with a 4.0 kHz uncertainty, as determined by the spectrometer used

The intensity variation shown in Figure 2.1 was considered. The peak responsible for the transition $6_{15} - 6_{06}$ was identified as the dimer (CO_2 / DFE) from earlier spectra.[4] For the vinyl fluoride (VF) and CO_2 studies, trimer VF / $(CO_2)_2$ intensities were of $\sim 1 - 10\%$ its dimer,[5] also, for this project the first guess for this peak pattern was a trimer (three molecules in any combination of CO_2 and DFE). Then the constant difference patterns needed to be identified. So far only a manual method was used to identify the constant difference patterns. MS Excel was helpful to some extent to identify the patterns, but not completely successful because the adjacent peaks ($1^{st} - 2^{nd}$, $3^{rd} - 4^{th}$) could lie below a 4 kHz range because of the uncertainty of the transitions, and that uncertainty is hard to feed into MS Excel. Using the manual method three constant difference patterns were identified. The frequency differences of the midpoints of the constant difference patterns are almost the same (~ 1096 MHz), indicating that they belong to one spectrum of the same cluster (Figure 2.2).

Table 2.1 - Frequencies of constant difference patterns. The distancing is ~2C between two constant difference patterns and that distance is very clear in the higher frequencies

P1 (MHz)	P2 (MHz)	P3 (MHz)	P4 (MHz)	P1 – P2 (d1) (MHz)	P3 – P4 (d2) (MHz)	d1 – d2 (MHz)	Mid-point (MHz)
7900.1222	7900.0466	7899.6956	7899.6158	0.0756	0.0798	0.0043	7899.8711
6804.4463	6804.0155	6802.0390	6801.6093	0.4308	0.4298	0.0010	6803.0273
5713.3763	5710.9705	5701.9091	5699.5027	2.4058	2.4064	0.0006	5706.4398
4634.4095	4622.9423	4593.9631	4582.4968	11.4672	11.4663	0.0009	4608.4527
3560.8956	3520.4469	3470.1992	3429.7492	40.4487	40.4500	0.0013	3495.3231

Distortion constants were applied since the structures are rotating with high J values, and do not behave as a rigid rotor and the bond lengths elongate. The frequency difference between d1 and d2 does not vary as it maintains the same energy

difference (Figure 2.3), which is equal to the energy difference of $5_{24} - 5_{14}$, so d1 =
d2. If two pairs of peaks are placed at the same distances within the ± 4 kHz margin,
those peaks are related to d1 and d2 - type difference in energy transitions. Three such
fingerprint-like constant difference patterns were identified around 7900 MHz, 6803
MHz and 5700 MHz (Table 2.1). Then using SPFIT application, the three
experimental rotational constants were obtained (Figure 2.4).[9,10] A total of 113
transitions were measured to obtain the experimental rotational constants with five
distortion constants (Table 2.2 & Table 2.3).

Table 2.2 - Experimental rotational and distortion constants of possible tetramer structure

Parameter	Experimental values
A / MHz	638.36285(11)
B / MHz	608.12956(12)
C / MHz	548.61474(11)
Δ_J / kHz	0.2641(21)
Δ_{JK} / kHz	0.218(9)
Δ_K / kHz	0.031(8)
δ_J / kHz	0.0506(11)
δ_K / kHz	-0.149(6)
$\Delta v_{rms}{}^a$ / kHz	2.3
N	113

$^a \Delta v_{rms} = \left(\frac{\Sigma(v_{obs}-v_{calc})^2}{N}\right)^{1/2}$; N is the number of transitions.
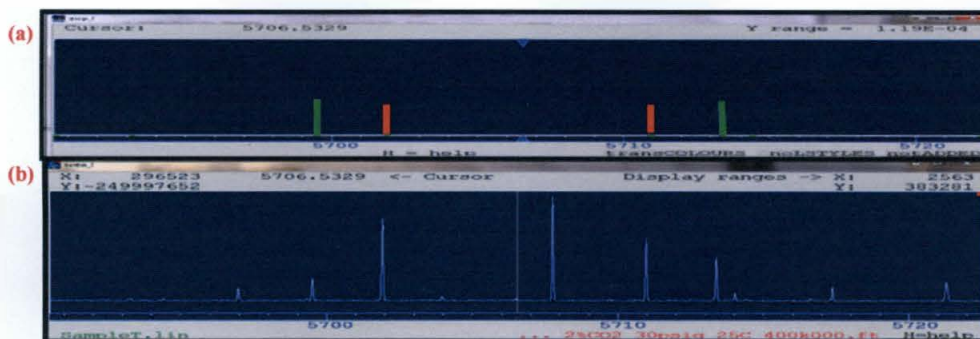
Figure 2.4 - Spectroscopic assignment of DFE / (CO₂)₃ tetramer using AABS and SPFIT/SPCAT programs. The predicted spectrum (Figure 2.4 (a)) and experimental rotational spectrum (Figure 2.4 (b)). Transitions are (left to right) ($J_{K_aK_c}$) : $5_{14} - 4_{23}, 5_{24} - 4_{23}, 5_{14} - 4_{13}, 5_{24} - 4_{13}$

Table 2.3 - Fitted rotational transitions of the identified spectrum

J'	K_a'	K_c'	J''	K_a''	K_c''	Exp. (MHz)	Exp. − Calc. (kHz)
2	0	2	1	1	1	2245.0458	-0.2
2	1	2	1	1	1	2253.9675	2.0
2	0	2	1	0	1	2275.2794	0.6
2	1	2	1	0	1	2284.1987	0.5
2	1	1	1	1	0	2372.9943	1.2
2	2	1	1	1	0	2463.6916	2.1
2	2	0	1	1	0	2501.8966	5.7
3	0	3	2	1	2	3359.6119	0.0
3	1	3	2	1	2	3361.3455	0.3
3	0	3	2	0	2	3368.5317	0.4
3	1	3	2	0	2	3370.2646	0.0
3	1	2	2	2	1	3429.7492	-2.3
3	2	2	2	2	1	3470.1992	0.0
3	1	2	2	1	1	3520.4469	-1.0
3	2	2	2	1	1	3560.8956	0.0
3	2	1	2	2	0	3571.8738	1.5
3	2	1	2	1	1	3700.7706	0.5
3	1	2	2	0	2	3707.9030	-6.9
3	3	1	2	2	0	3751.5238	-2.6
3	3	0	2	2	1	3809.1579	-2.3
3	3	0	2	1	1	3899.8533	-3.4
4	0	4	3	1	3	4461.0735	-0.3
4	1	4	3	1	3	4461.3511	0.0
4	0	4	3	0	3	4462.8061	-1.1
4	1	4	3	0	3	4463.0856	1.1
4	2	2	3	3	1	4570.1544	5.4
4	1	3	3	2	2	4582.4968	1.8
4	2	3	3	2	2	4593.9631	-0.1
4	1	3	3	1	2	4622.9423	-0.1
4	2	3	3	1	2	4634.4095	-1.3

J'	K'_a	K'_c	J''	K''_a	K''_c	Exp. (MHz)	Exp. – Calc. (kHz)
4	3	2	3	3	1	4673.4326	0.0
4	2	2	3	2	1	4749.8029	-0.1
4	3	1	3	3	0	4749.8759	-1.2
4	3	2	3	2	1	4853.0864	-0.5
4	2	2	3	1	2	4930.1265	1.3
4	3	1	3	2	1	4948.9620	-1.8
4	2	3	3	1	3	4972.0571	0.8
4	3	2	3	2	2	4992.9595	-1.8
4	4	1	3	3	0	5040.7103	0.7
4	4	0	3	3	0	5048.9726	0.6
4	4	1	3	3	1	5060.1409	-1.1
4	4	0	3	3	1	5068.4082	3.6
4	3	1	3	1	2	5129.2872	1.2
4	4	0	3	2	1	5248.0607	2.0
4	4	1	3	2	2	5379.6691	-1.6
5	3	2	4	4	0	5659.6641	-1.5
5	1	4	4	2	3	5699.5027	0.6
5	2	4	4	2	3	5701.9091	1.1
5	1	4	4	1	3	5710.9705	0.1
5	2	4	4	1	3	5713.3763	0.0
5	2	3	4	3	2	5775.3660	1.6
5	3	3	4	3	2	5816.2680	0.7
5	4	2	4	4	1	5865.2298	2.3
5	2	3	4	2	2	5878.6477	-0.4
5	4	1	4	4	0	5912.7671	0.9
5	3	3	4	2	2	5919.5511	0.0
5	3	2	4	3	1	5958.7613	0.8
5	4	2	4	3	1	6156.0594	-0.3
5	3	2	4	2	2	6157.9176	-3.6
5	2	3	4	1	3	6185.8316	0.7
5	4	1	4	3	1	6211.8604	-0.5
5	2	4	4	1	4	6212.6096	-3.4
5	3	3	4	2	3	6215.2658	0.3
5	4	2	4	3	2	6251.9353	-1.4
5	4	1	4	3	2	6307.7367	-1.2
5	5	1	4	4	0	6325.2507	-1.4
5	5	0	4	4	0	6328.3899	1.5
5	5	1	4	4	1	6333.5139	-0.7
5	5	0	4	4	1	6336.6498	-1.0
5	4	1	4	2	2	6411.0215	-0.1
5	3	2	4	2	3	6453.6375	1.8
5	3	2	4	1	3	6465.1049	0.9
5	5	0	4	3	1	6627.4893	6.0
5	4	2	4	2	3	6650.9290	-5.8
5	5	1	4	3	2	6720.2203	-3.6

J'	K_a'	K_c'	J''	K_a''	K_c''	Exp. (MHz)	Exp. – Calc. (kHz)
6	4	2	5	5	1	6731.7552	-5.9
6	1	5	5	2	4	6801.6093	0.2
6	2	5	5	2	4	6802.0390	2.1
6	1	5	5	1	4	6804.0155	0.5
6	2	5	5	1	4	6804.4463	3.5
6	3	3	5	4	1	6869.3015	-5.7
6	3	3	5	4	2	6925.1098	1.3
6	2	4	5	3	3	6926.3315	0.2
6	3	4	5	3	3	6937.5827	0.3
6	2	4	5	2	3	6967.2348	0.6
6	4	3	5	4	2	7026.6567	0.5
6	5	2	5	5	1	7048.2338	2.5
6	5	1	5	5	0	7072.7021	0.8
6	3	3	5	3	2	7122.4070	-0.6
6	4	2	5	4	1	7144.2480	0.7
6	4	3	5	3	2	7223.9533	-2.1
6	4	2	5	3	2	7397.3476	0.0
6	3	3	5	2	3	7401.6802	-0.6
6	2	4	5	1	4	7442.0987	4.1
6	3	4	5	2	4	7450.9393	-0.5
6	5	2	5	4	1	7460.7160	-1.2
6	4	3	5	3	3	7462.3258	0.1
6	5	1	5	4	1	7488.3231	-0.4
6	5	2	5	4	2	7516.5173	-1.1
6	5	1	5	4	2	7544.1230	-1.6
6	6	1	5	5	0	7605.4862	-2.8
6	6	0	5	5	0	7606.5996	1.0
6	6	1	5	5	1	7608.6233	-2.0
6	6	0	5	5	1	7609.7348	0.0
6	4	2	5	3	3	7635.7199	2.0
6	4	2	5	2	3	7676.6203	-0.4
6	5	1	5	3	2	7741.4272	3.2
6	3	3	5	2	4	7874.1415	6.1
6	3	3	5	1	4	7876.5407	-0.6
7	1	6	6	2	5	7899.6158	-5.4
7	2	6	6	2	5	7899.6956	5.6
7	1	6	6	1	5	7900.0466	-2.4
6	4	3	5	1	4	7978.0907	1.6

2.3 Computational analysis (Theoretical)

ABCluster and manual arrangements were used to deduce the structure and the calculations were optimized from Gaussian09W at ωB97X-D/6-31+G(d,p) level.[11]

ABCluster is an application that does basic structure identification using the Coulomb-Lennard-Jones potential.[12,13] ABCluster acts as an artificial bee colony which identifies the lowest energy structure and seeks (like a bee looking for better nectar) another structure which is lower than the previously identified structure. When initiating this method, the group was doubtful about the accuracy of the application. However, the first tests were done on previously identified structures to check whether it can reproduce the previous data, such as DFE / CO_2 dimer structures. While the computational parameters were varied, the output structures were observed and with the final applied parameters, ABCluster gave the expected DFE / CO_2 lowest energy structure which was theoretically calculated and experimentally observed.[4] This is a simple approximation which is not adequate to obtain the final structures, but the ABCluster output structures arrange the molecules to the close proximity of the lowest energy structure. Hence it reduces the optimization time for *ab initio* calculations.

Ab initio calculations were done using Gaussian09W at ωB97X-D/6-31+G(d,p) level to optimize the theoretical structures which were obtained from the manual method or from ABCluster. For the manual arrangement, previous DFE / CO_2 stable theoretical structural arrangements were considered.[4] Also known were the rotational constants of the DFE / CO_2 dimer. The dimer rotational constant values numerically were much larger than compared to the new experimental rotational constants, so the structural optimization was started with trimers (DFE / $(CO_2)_2$) (Table 2.4), and then expanded to optimize tetramers and pentamers. The experimental values were most comparable with a tetramer structure. However, for each combination (trimer, tetramer, pentamer, etc.) more than twenty different structural arrangements were optimized within the lowest energy arrangements shown

in Figure 2.5 – 2.7. Then for all the structures, the difference between the average of the experimental and the theoretical rotational constants was calculated (Equation 2.1). This value gives an idea of the deviation of the theoretical values from the experimental values (Table 2.5). As it was a single value, it is easy to understand there would be a deviation. It is assumed that the cluster giving the minimum simple difference was probably the cluster responsible for the experimental values.

$$Simple\ difference = \left(\left(\frac{A+B+C}{3}\right)_{Experimental} - \left(\frac{A+B+C}{3}\right)_{Theoretical}\right) \qquad (2.1)$$

Table 2.4 – Comparison of experimental spectroscopic data and the lowest energy theoretical structural data

Parameters	Experimental values	Trimer 1 DFE / $(CO_2)_2$	Tetramer 1 DFE / $(CO_2)_3$	Pentamer $(DFE)_2$ / $(CO_2)_3$
A / MHz	638.36285(11)	1122	634	422
B / MHz	608.12956(12)	991	581	341
C / MHz	548.61474(11)	604	532	264
μ_a / D	strong	0.5	0.9	0.1
μ_b / D	weakest	1.1	1.0	0.1
μ_c / D	weak	0.9	0.1	0.1
P_{aa} / amu $\mathrm{\AA}^2$ [a]	480.2748(5)	448.1	511.0	1101.1
P_{bb} / amu $\mathrm{\AA}^2$	440.9163(5)	388.6	439.5	813.1
P_{cc} / amu $\mathrm{\AA}^2$	350.7636(5)	61.9	358.1	382.8
$\%\Delta B_{avg}$		51.4	2.69	129.7
Δv_{rms} [c] / kHz	2.3			
N	113			

[a] Planar moment $P_a = 0.5(I_b + I_c + I_a) = \Sigma_i m_i r_i^2$

[b] Percent difference between experimental and calculated rotational constants of each sized cluster. $(B_x = A, B, C)$ $(\%\Delta B_{avg} = (\Sigma(B_x(obs)-B_x(calc)/B_x(obs)) \times 100\%)$.

[c] $\Delta v_{rms} = \left(\frac{\Sigma(v_{obs}-v_{calc})^2}{N}\right)^{1/2}$; N is number of transitions of the spectrum.

Table 2.5 - The difference of the average of the experimental rotational constants and theoretical rotational constants of the lowest energy structures

	A (MHz)	B (MHz)	C (MHz)	Simple Difference
Experimental	638.36285(11)	608.12956(12)	548.61474(11)	0
Theoretical Trimer	1122	991	604	307
Theoretical Tetramer	634	581	532	-16
Theoretical Pentamer	422	341	264	256
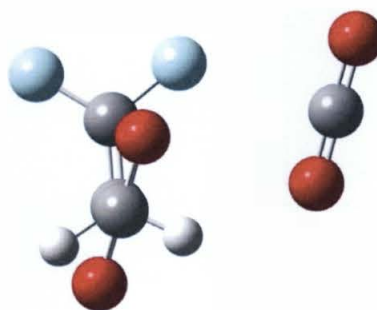
Figure 2.5 - The lowest energy DFE / $(CO_2)_2$ trimer
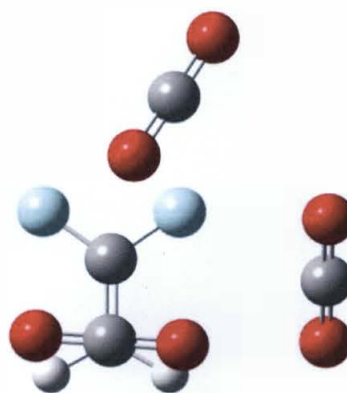
Figure 2.6 - The lowest energy DFE / $(CO_2)_3$ tetramer

Figure 2.7 - The lowest energy (DFE)$_2$ / (CO$_2$)$_3$ pentamer

When comparing the theoretical structures to the experimental structure, there is no doubt that the experimental values belong to a tetramer structure, so thereafter different tetramer orientations were optimized to find the best structure.

2.4 Tetramer optimization

After the confirmation of the cluster composition as a tetramer (DFE / (CO$_2$)$_3$), different tetramer orientations were optimized using Gaussian09W at ωB97X-D/6-31+G(d,p) level. Then the theoretical values of the tetramer structures were compared to experimental values to identify the best match. The structures were compared visually with the components of the dimer structures (Table 2.6) and the theoretical values were compared with the experimental values as well (Table 2.7). First the %ΔB_{avg} and ΔE (the energy difference of the particular structure's energy and the minimum energy structure in kJ/mol) were considered. However, the P_{aa}, P_{bb} and P_{cc} parameters were also considered. But in comparison to the DFE / CO$_2$ dimer structure, the planar moment values are harder to relate directly to observed structural features as the structures are getting bulkier.

Table 2.6 - Energies and the relative energies of the theoretically stable structures of DFE / $(CO_2)_3$ tetramer. The optimization was done in Gaussian09W at ωB97X-D/6-31+G(d,p) level. (TT1 denotes the stable theoretical structure of DFE / $(CO_2)_3$ tetramer)
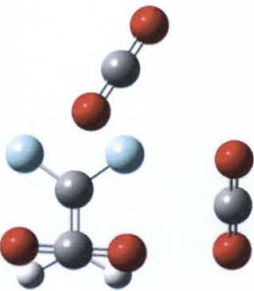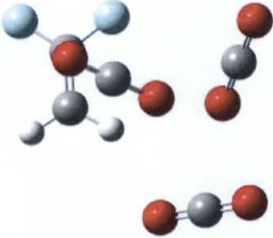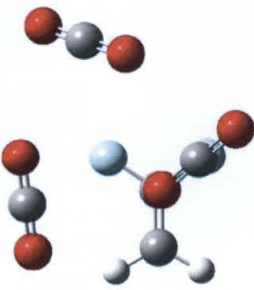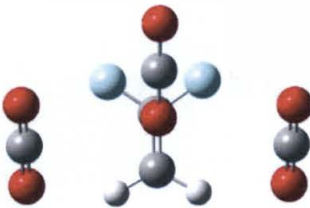
Structure	Energy (E_h)	Relative energy (Energy – Min. Energy) (kJ/mol)
(TT1) – b08	-842.58986	0.00
(TT2) - b12	-842.58925	1.59
(TT3) – b15	-842.58875	2.91
(TT4) – b09	-842.58866	3.15

Table 2.7 - The comparison of experimental spectroscopic data with theoretical data of low energy tetramer structures

Parameters	Experimental values	TT1[a]	TT2	TT3	TT4
A / MHz	638.36285(11)	634	631	616	797
B / MHz	608.12956(12)	581	585	575	485
C / MHz	548.61474(11)	532	533	494	380
μ_a / D	strong	0.9	1.0	1.4	0.0
μ_b / D	weakest	1.0	0.9	0.2	1.0
μ_c / D	weak	0.1	0.1	0.6	1.2
P_{aa}/ amu $\mathring{A}^2$	480.2748(5)	511.0	505.3	540.2	869.2
P_{bb}/ amu $\mathring{A}^2$	440.9163(5)	439.5	442.1	481.9	461.8
P_{cc}/ amu $\mathring{A}^2$	350.7636(5)	358.1	358.6	338.8	172.0
$\%\Delta B_{avg}$		2.7	3.0	6.1	7.4
ΔE (kJmol^{-1})[b]		0.00	1.59	2.91	3.15

[a] TT1 denotes the stable theoretical structure of DFE / $(CO_2)_3$ tetramer.

[b] E, Energy is calculated from the DFT when it is optimized at ωB97X-D/6-31+G(d,p) level. ΔE is the energy difference of the particular structure's energy and the minimum energy structure.

2.5 Theoretical structure optimization and interpretation

The theoretical structure optimization was done by two methods.

1. Manual arrangement
2. ABCluster

Manual arrangement

Experimental and theoretical structural studies of the DFE / CO_2 dimer have been previously done,[4] so it is fair to think that the tetramer contains the dimer arrangements. In the dimer studies, four theoretically stable structures were identified

but only one structure was experimentally found (Figure 2.8). It is believed that the formation of the other three structures were not favorable at this condition, so in the manual arrangement, the DFE and CO_2 molecules were arranged first as in the dimer, and then a tetramer arrangement was built around the dimer fragment.

	I	II	III	IV
ΔE (kJmol^{-1})	0.00	0.25	0.56	0.60
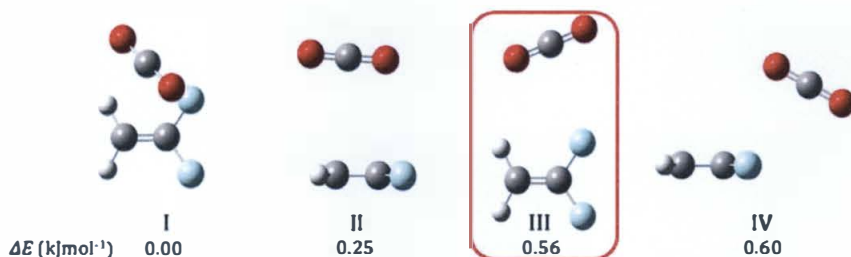
E, Energy is calculated from zero-point energy (ZPE) at MP2/6-311++G(2d,2p) level when it is optimized. ΔE is the energy difference of the particular structure's energy and the minimum energy structure.

Figure 2.8 - Previously identified theoretical DFE / CO_2 dimer orientations. Only structure III was experimentally identified[4]
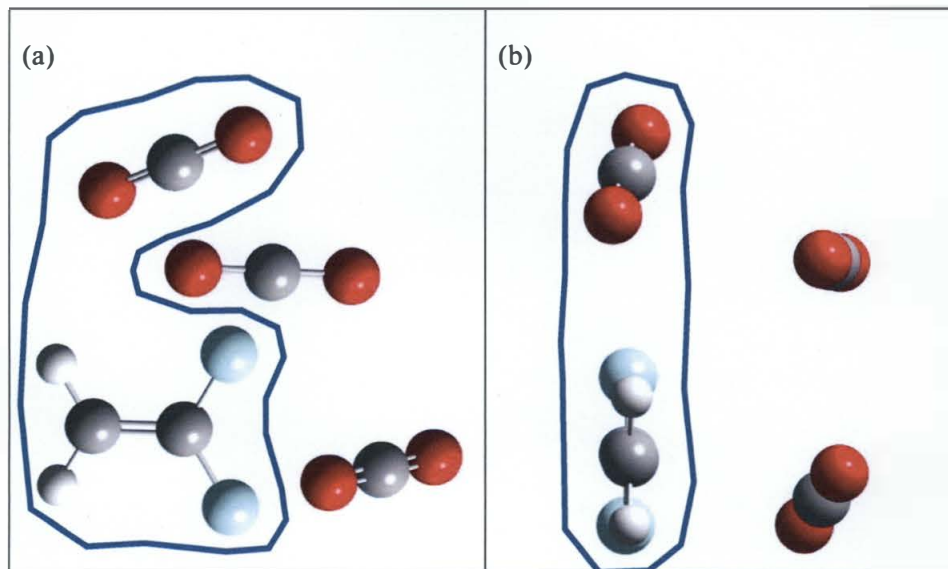
Figure 2.9 – (a) Initial structural arrangement of DFE / $(CO_2)_3$ with the orientations from the dimer structures. (b) The side-view of (a). The encircled molecules are very similar to DFE / CO_2 dimer structure

The method showed a considerable level of success as most of the structures resulted in arrangements very similar to the dimer orientation. But there were two limitations. First, there might be stable arrangements at completely different positions that are difficult to imagine. Secondly, when the structure gets bigger, it is harder to

34

arrange the molecules in 3D structures logically while paying attention to the attractions and repulsions of all the atoms, so it was necessary to find a better structure deducing method, and here ABCluster was used.

ABCluster

ABCluster is a method of predicting stable (low energy) structures of loosely bound complexes and ions by using Coulomb-Lennard-Jones potential (Equation 2.2).[12,13] This equation gives the potential energy using three parameters; q, the relative charge of an atom, σ ($\dot{A}$) the equilibrium distance when the potential energy is minimum among two atoms, and ϵ (kJ mol^{-1}) the depth of the potential well (when the σ is at its lowest).

$$U_{LJ} = \sum_{i=1}^{N} \sum_{i<j}^{N} \left(\frac{q_i q_j}{r_{ij}} + 4 \in_{ij} \left(\left(\frac{\sigma_{ij}}{r_{ij}} \right)^{12} - \left(\frac{\sigma_{ij}}{r_{ij}} \right)^{6} \right) \right) \qquad (2.2)$$

ABCluster is also known as Artificial Bee Colony; the term was used because it acts like a bee colony. Bees in a beehive need to find the best nectar source around, so for that, they effectively communicate the information about the nectar to other bees using their 'waggle dance'; first they find a nectar source and communicate it to the other bees, so the other bees use that nectar and also look for other nectar sources as well. When they find another source of nectar, they compare the quality of the nectar to that of the previously found sources, choosing the best one and removing the other sources. This cycle is repeated until they find the best source of nectar.

Likewise, in ABCluster, first it finds a stable structure with low potential energy ($U_{(x)}$) of a structure in the pool of structures. Then it looks for other structures which have lower energy than the previous one. When it finds a lower energy one, it

35

takes that structure while removing the higher energy structure. Then the cycle runs again looking for even lower energy structures. After running for many cycles, it finds the lowest energy structure.

The input for this calculation needs the charge (q, Coulomb), epsilon (ϵ, kJ/mol) and sigma (σ, $\dot{A}$). Charge is assigned to atoms assuming a +1 cation has a +1 charge and a -1 anion has -1 charge. As DFE and CO_2 molecules do not have an external charge, all the charges contain values in between $-1 < q < 1$. Also, as CO_2 and DFE do not have an external charge, the sum of the charges of each molecule should be zero. Luckily, for CO_2 the data was easily available as the newest force field data can be downloaded from *http://mackerell.umaryland.edu/charmm ff.shtml*.[14] Likewise, the σ and ϵ values for the two molecules can also be found from the manual. Fortunately, the force field values for CO_2 were available in the manual, but for DFE the values had to be estimated, after finding somewhat similar molecules. As an example, the σ and ϵ values (but not q) for F in fluoroethene were not available, but the fluoroethane values, which are available could be used. It is true that these structures are different so force field values would be different. However, toppar/top_all36_cgenff.rtf file in the resources, provides the q value for aliphatic fluoroalkane and its charge is equal to -0.22 C and that molecule is the simplest molecule which has fluorine in it (#FGA1) (Figure 2.10), so it is fair to assume that fluorine in this DFE molecule will also take a closer value to -0.22 C. Then the code FGA1 was taken and that code is used to find σ and ϵ values for the fluorine atom (from fluoroethane) in toppar/par all36 cgenff.rtf.

```
ATOM H12'  HGA2      0.09
ATOM C4'   CG3C51    0.11 !       H52'  H53'
ATOM H42'  HGA1      0.09 !         \  /
ATOM C2'   CG3C51    0.05 !     H51'-C5'   04'   H11'
ATOM H22'  HGA6      0.11 !         \  / \  /
ATOM F2'   FGA1     -0.22 !       H42'--C4'   C1'--H12'
ATOM C3'   CG3C51   -0.06 !          |       |
ATOM H31'  HGA1      0.09 !       H31'--C3'--C2'--F2'  (beta)
GROUP                     !         /         \
ATOM O3'   OG303    -0.40 !       O3'          H22'
ATOM P     PG2       1.10 !        |
ATOM O1P   OG2P1    -0.90 !     O1P==P==O2P
ATOM O2P   OG2P1    -0.90 !         ||
ATOM O3P   OG2P1    -0.90 !         O3P  (-2)
GROUP
ATOM C5'   CG331    -0.27
ATOM H51'  HGA3      0.09
ATOM H52'  HGA3      0.09
ATOM H53'  HGA3      0.09
```
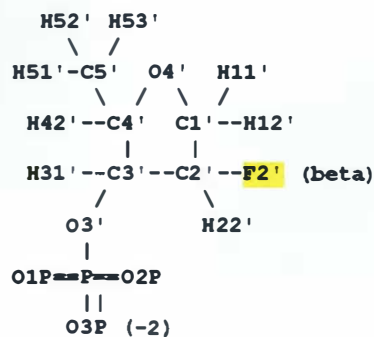
Figure 2.10 - The available fluoroalkane in the ABCluster resource, its code and the charge[15]

Thereafter σ and ε need to be converted using the given equations 2.3 – 2.4.

$$\epsilon_{ABCluster} = \epsilon_{CHARMM} \times (-4.184) \tag{2.3}$$

$$\sigma_{ABCluster} = \sigma_{CHARMM} \times 2^{5/6} \tag{2.4}$$

Using different guessing parameters, ABCluster was run on the DFE / CO_2 dimer, a structure that was previously identified theoretically and experimentally, so the parameters were changed until ABCluster gave an output similar to the experimentally found dimer structure and finally it gave the correct dimer structure. These final parameters were then used in this study. They still might not be the best parameters, but as it provides a very similar structure to the identified DFE / CO_2 dimer, it is believable that the parameters are accurate to a certain level. To make the parameters better, the resulting structures have been optimized using Gaussian09W. But the better output is still expected because parameters used for ABCluster have given very similar outputs to the experimentally and theoretically identified DFE / CO_2 structure and even in the identified theoretical trimer and tetramer structures, the dimer structural components can be seen. Also, it is very efficient in providing 60 or

more structures in less than a few seconds. Moreover, the given values are further optimized by Gaussian09W.

ABCluster needs three types of input files to run its application; a .xyz file for each molecule; an .inp file, and a .cluster file. The cluster file contains information about the composition of the cluster. For example, for the tetramer, it consists of 2 different types of molecules (DFE and CO_2) and 1 of DFE and 3 of CO_2 are required to make the cluster (Figure 2.11). Then the .inp file is required (Figure 2.12). It contains information about how many local minima (LM) are to be saved and what cluster file values to use.

.Cluster file
2 ⟵──────────── # of different molecules/ .xyz files
dfe.xyz 1⟵──────────── # of DFE in the cluster
co2.xyz 3 ⟵──────────── # of CO_2 in the cluster
* 10.0000

Figure 2.11 - Cluster file for DFE / $(CO_2)_3$ tetramer

.inp file
D1C3.cluster   # cluster file name
20   # population size
100   # maximal generations
3   # scout limit
10.00000000   # amplitude
D1C3   # save optimized configuration
60   # number of LMs to be saved

Figure 2.12 - .inp file for DFE / $(CO_2)_3$ tetramer

The last file is the .xyz file. For each different molecule it needs a .xyz file, hence here it needs .xyz files for CO_2 and DFE (Figure 2.13 & 2.14). For CO_2 the .xyz was available in the resources. But for DFE, a closely related molecule's values were used (see above). These structures are more accurately optimized by Gaussian09W in ωB97X-D/6-31+G(d,p) format. At the moment, a brief optimization is necessary, so

even though all the true forcefield values were not used, it appears to be okay to use the ABCluster output files as the input of Gaussian09W to optimize.

The other thing that must be considered in order to obtain reliable ABCluster result is the charge of each atom according to its distribution of electrons. It is assumed that one + ion has +1 charge and with that assumption, the values were assigned roughly as the electronic charge expected to be distributed in the molecule. In the latter part of the file content, the tag is for the value of ϵ and σ values. From the tag, the source can be found as described above and in Figure 2.10.

CO2.xyz file
3 -- # atoms in the molecule
carbon dioxide
C 0.00000000 0.00000000 0.00000000 ⎤
O 0.00000000 0.00000000 1.162   ⎬ xyz coordinates of each atoms
O 0.00000000 0.00000000 -1.162   ⎦

q (C) ϵ (kJ/mol) σ ($\dot{A}$)
+0.60   0.2427   2.7849 # CG2O7 ⎤
-0.30   0.6904   3.0148 # OG2D5 ⎬ q, ϵ and σ values for each atom
-0.30   0.6904   3.0148 # OG2D5 ⎦

Figure 2.13 - The content of the xyz file of CO_2

DFE.xyz file
6
difluoroethylene
C -0.17222200   1.35232000   0.00000000
H -1.15770300   1.76912800   0.00000000
H 0.68020500   1.99905600   0.00000000
C 0.00000000   0.00810800   0.00000000
F 1.24336300   -0.51777200   0.00000000
F -1.07549200   -0.80786800   0.00000000
q (C) ϵ (kJ/mol) σ ($\dot{A}$)
 -0.26   0.2678   3.7061 # CG2D2
+0.17   0.1088   2.2451 # HGA4
+0.17   0.1088   2.2451 # HGA4
+0.55   0.2678   3.7061 # CG2D2
- 0.32   0.4058   2.8509 # FGA1
- 0.31   0.4058   2.8509 # FGA1

Figure 2.14 - The content of the xyz file of DFE

Using the data set for fluoroethane (DFE_1) (Figure 2.15), for ABCluster did not give the expected structure (Figure 2.16), so the q values were changed until it gave the correct structure (DFE_2) (Figure 2.17) and the global minimum of the dimer was obtained (Figure 2.18).[12,13] Hence it was assumed the data set (q, σ, and ϵ) was correct and good to use for further calculations for trimer and beyond.

DFE.xyz (DFE_1)

6

difluoroethylene

C -0.17222200 1.35232000 0.00000000

H -1.15770300 1.76912800 0.00000000

H +0.68020500 1.99905600 0.00000000

C +0.00000000 0.00810800 0.00000000

F +1.24336300 -0.51777200 0.00000000

F -1.07549200 -0.80786800 0.00000000

q (C)	ϵ (kJ/mol)	σ (Å)	
- 0.26	0.2678	3.7061	# CG2D2
+0.10	0.1088	2.2451	# HGA5
+0.10	0.1088	2.2451	# HGA5
+0.55	0.2678	3.7061	# CG2D2
- 0.32	0.4058	2.8509	# FGA1
- 0.31	0.4058	2.8509	# FGA1

Figure 2.15 - 1st .xyz file data for DFE with the initial q values
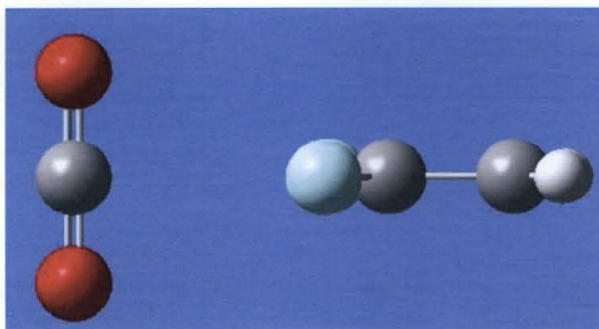
Figure 2.16 - First DFE / CO_2 structure obtained from ABCluster

DFE.xyz (DFE_2)
6
difluoroethylene
C -0.17222200   1.35232000   0.00000000
H -1.15770300   1.76912800   0.00000000
H +0.68020500 1.99905600   0.00000000
C +0.00000000 0.00810800   0.00000000
F +1.24336300 -0.51777200   0.00000000
F -1.07549200   -0.80786800   0.00000000
q (C)   ϵ (kJ/mol)   σ (Å)
- 0.50   0.2845   3.7240 # CG2D2
+0.25   0.1088   2.2451 # HGA5
+0.25   0.1088   2.2451 # HGA5
+0.60   0.2845   3.7240 # CG2D2
- 0.30   0.4058   2.8509 # FGA1
- 0.30   0.4058   2.8509 # FGA1

Figure 2.17 - Corrected .xyz file for DFE with new q values
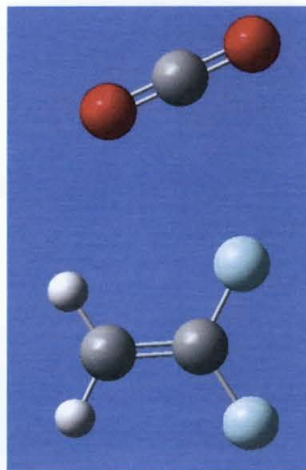
Figure 2.18 - Expected dimer structure (DFE / CO_2)

When the application is run, it provides .gjf files (60 or more as requested). Each .gjf file contains the approximately optimized (from Coulomb-Lennard-Jones potential energy equation) xyz coordinates of all the atoms. Also, the graphical interpretation of this could be obtained using GaussView (Figure 2.19).
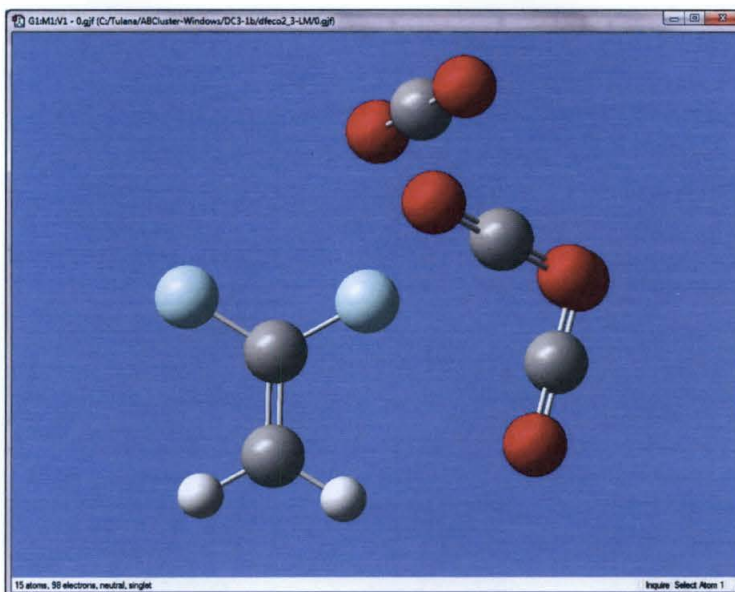
Figure 2.19 - Graphical interface of the .gjf file of the 0th structure of DFE / $(CO_2)_3$. (In ABCluster, the lowest energy structure is given as 0th structure)

The .gjf file is then further optimized with Gaussian09W using the ωB97X-D/6-31+G(d,p) format. For this structure, it took 1 hour and 36 minutes to optimize (Figure 2.20). It could be said that due to ABCluster's initial preliminary calculations, the optimization time in Gaussian09W is also reduced compared to the time taken to optimize a manually oriented structure. ABCluster is only a tool for very preliminary level optimization. But when Gaussian09W is for this calculation, the structures are optimized with the density functional theory (DFT), so it is fair to expect a somewhat different structure than the input.
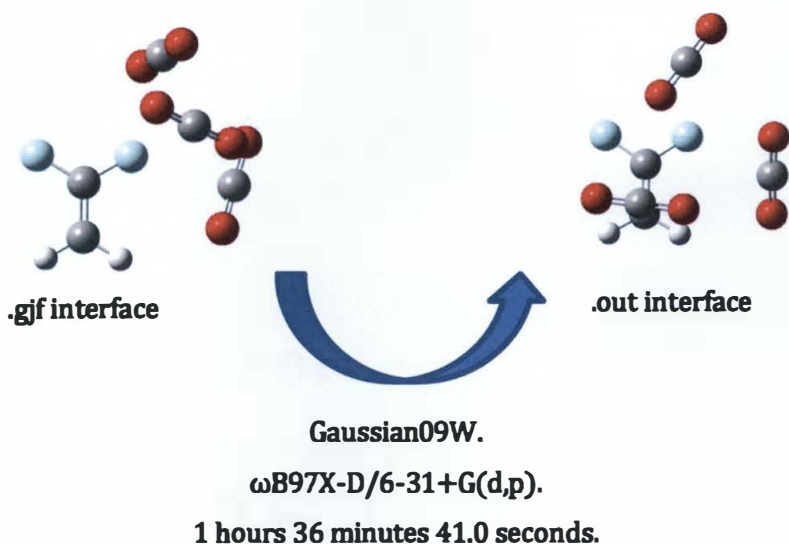
Figure 2.20 – Gaussian09W optimization of .gjf file

With the details obtained, the 0th structure is the best fitting theoretical structure for the found spectrum. For the DFE / $(CO_2)_3$ tetramer, 20 structures were optimized using the manual structural arrangement, while 40 structures were optimized using ABCluster. The lowest energy structure given from all of the above after Gaussian09W optimization, was not the 0th structure (given by ABCluster), but the 8th structure. However, the 0th structure and the 8th structures are visibly very similar, and the energy difference between them is 25.9 J mol^{-1} (Table 2.8). Also, the %ΔB_{avg} value is lower in the 0th structure (2.69 MHz). Hence 0th structure can be taken as the best matching structure with the experimental data. It is not an uncommon thing of observing repetitions of structures in the output of ABCluster. Such structures can gives two different energy values because of the error associated with the optimization method.

(a)   (b)
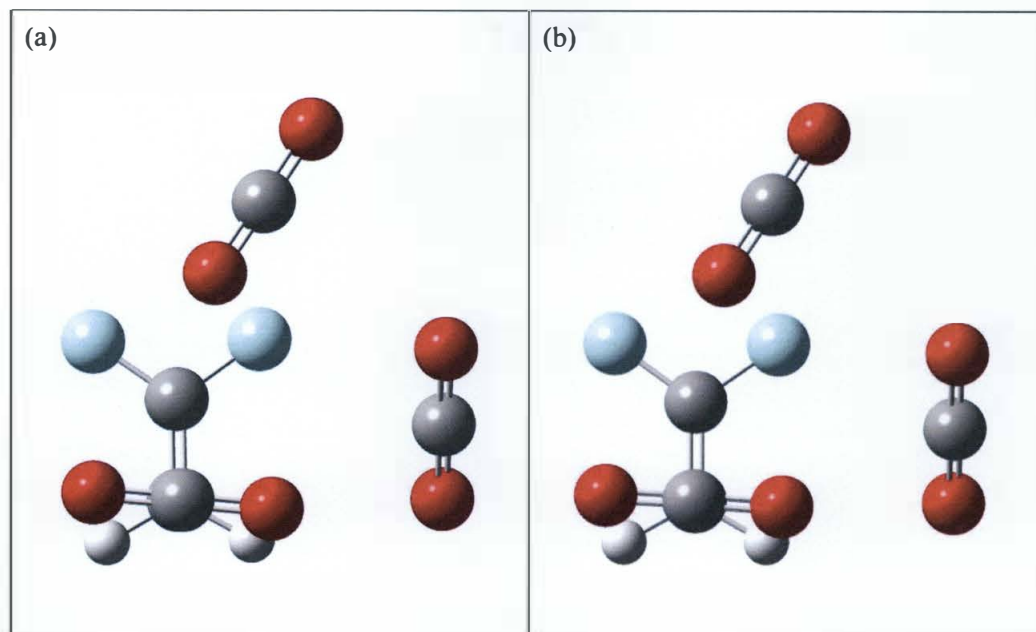
Figure 2.21 – (a) Best fitting structure (Tetramer, DFE / (CO₂)₃) for the found spectrum, (b) 8ᵗʰ structure from ABCluster after the optimization – the 8ᵗʰ structure is essentially the same as the 0ᵗʰ structure

Table 2.8 - Theoretical data comparison of 0th structure vs. 8th structure

Parameters	0th structure theoretical values	8th structure theoretical values
A / MHz	634	626
B / MHz	581	585
C / MHz	532	530
μ_a / D	0.9	1.0
μ_b / D	1.0	0.9
μ_c / D	0.1	0.1
P_{aa} / amu Å^2	511.0	505.0
P_{bb} / amu Å^2	439.5	448.4
P_{cc} / amu Å^2	358.1	358.6
$\%\Delta B_{avg}$	2.7	3.0
ΔE (J mol^{-1})	0.0	25.9

44

In this structure identification and optimization, it was confirmed that the found experimental structurer is a tetramer (DFE / $(CO_2)_3$), even though it was initially expected to be a trimer. But the experimental rotational constants are very different from the trimer values. The structure optimization was done using both the manual method and using ABCluster. From all the methods, finally, the most closely comparable structure was identified as the 0th structure which was obtained from ABCluster and optimized.

References

[1] Raveendran, P.; Ikushima, Y.; Wallen, S. L. Polar attributes of supercritical carbon dioxide. *Acc. Chem. Res.* **2005**, *38*, 478.

[2] Bemish, R. J.; Block, P. A.; Pedersen, L. G.; Miller, R. E. The ethylene–carbon dioxide complex: A double internal rotor. *J. Chem. Phys.* **1995**, *103*, 7788.

[3] Christenholz, C. L.; Dorris, R. E.; Peebles, R. A.; Peebles, S. A. Characterization of Two isomers of the vinyl Fluoride—Carbon Dioxide complex. *J. Phys. Chem. A* **2014**, *118*, 8765.

[4] Anderton, A. M.; Peebles, R. A.; Peebles, S. A. Rotational Spectrum and Structure of the 1,1-Difluoroethylene···Carbon Dioxide Complex. *J. Phys. Chem. A* **2016**, *120*, 247.

[5] Brown, G. G.; Dian, B. C.; Douglass, K. O.; Geyer, S. M.; Shipman, S. T.; Pate, B. H. A broadband Fourier transform microwave spectrometer based on chirped pulse excitation. *Rev. Sci. Instrum.* **2008**, *79*, 053103.

[6] Origin 8.1 SR1. v8.1.13.88 (Academic). OriginLab corporation, Northampton 1060, MA. **1991 – 2009.**

[7] Kannangara, P. B.; West, C. T.; Peebles, S. A.; Peebles, R. A. Towards microsolvation of fluorocarbons by CO_2: Two isomers of fluoroethylene-$(CO_2)_2$ observed using chirped-pulse Fourier-transform microwave spectroscopy. *Chem. Phys. Lett.* **2018**, *706*, 538.

[8] Harrington, H. W.; Hearn, J. R.; Rauskolb, R. F. The routine rotational microwave spectrometer. Hewlett-Packard journal. **1971**, *2*, 2.

[9] Pickett, H. M. The Fitting and Prediction of Vibration-Rotation Spectra with Spin Interactions, *J. Mol. Spectrosc.* **1991**, *148*, 371.

[10] Kisiel, Z.; Pszczolkowski, L.; Medvedev, I. R.; Winnewisser, M.; De Lucia, F. C.; Herbst, E. Rotational Spectrum of Trans-Trans Diethyl Ether in the Ground and Three Excited Vibrational States. *J. Mol. Spectrosc.* **2005**, *233*, 231.

[11] Frisch, M. J.; Trucks, G. W.; Schlegel, H. B.; Scuseria, G. E.; Robb, M. A. Cheeseman, J. R.; Scalmani, G.; Barone, V.; Mennucci, B.; Petersson, G. A.; Nakatsuji, H.; Caricato, M.; Li, X.; Hratchian, H. P.; Izmaylov, A. F.; Bloino, J.; Zheng, G.; Sonnenberg, J. L.; Hada, M.; Ehara, M.; Toyota, K.; Fukuda, R.; Hasegawa, J.; Ishida, M.; Nakajima, T.; Honda, Y.; Kitao, O.; Nakai, H.; Vreven, T.; Montgomery, Jr., J. A.; Peralta, J. E.; Ogliaro, F.; Bearpark, M.; Heyd, J. J.; Brothers, E.; Kudin, K. N.; Staroverov, V. N.; Keith, T.; Kobayashi, R.; Normand, J.; Raghavachari, K.; Rendell, A.; Burant, J. C.; Iyengar, S. S.; Tomasi, J.; Cossi, M.; Rega, N.; Millam, J. M.; Klene, M.; Knox, J. E.; Cross, J. B.; Bakken, V.; Adamo, C.; Jaramillo, J.; Gomperts, R.; Stratmann, R. E.; Yazyev, O.; Austin, A. J.; Cammi, R.; Pomelli, C.; Ochterski, J. W.; Martin, R. L.; Morokuma, K.; Zakrzewski, V. G.; Voth, G. A.; Salvador, P.; Dannenberg, J. J.; Dapprich, S.; Daniels, A. D.; Farkas, O.; Foresman, J. B.; Ortiz, J. V.; Cioslowski, J.; Fox, D. J. Gaussian 09, Revision E.01, Gaussian, Inc., Wallingford CT, **2013.**

[12] Zhang, J.; Dolg, M. ABCluster: The Artificial Bee Colony Algorithm for Cluster Global Optimization. *Phys. Chem. Chem. Phys.* **2015**, *17*, 24173.

[13] Zhang, J.; Dolg, M. Global optimization of clusters of rigid molecules using the artificial bee colony algorithm. *Phys. Chem. Chem. Phys.* **2016**, *18*, 3003.

[14] Vanommeslaeghe, K.; Hatcher, E.; Acharya, C.; Kundu, S.; Zhong, S.; Shim, J.; Darian, E.; Guvench, O.; Lopes, P.; Vorobyov, I.; Mackerell, Jr., A. D. CHARMM general force field: A force field for drug-like molecules compatible with the CHARMM all-atom additive biological force fields. *J. Comput. Chem.* **2010**, *31*, 671.

[15] Zhang, J. ABCluster Manual. Version 1.5.1. http://www.zhjun-sci.com/software-abcluster-download.php.

Chapter 3

3. Experimental analysis of pure 1,1-difluoroethene (DFE) spectrum

3.1 Introduction

Apart from the mainstream study of mixtures of 1,1-difluoroethene (DFE) and CO_2, a sample of only 1,1-difluoroethene (DFE) was also analyzed at this time. These results do not directly give any conclusions about the solvation properties of CO_2 but the behavior of DFE in this spectrum will indeed help understand the behavior of DFE in DFE / CO_2 spectra. For example, the attraction and repulsion forces among F and F atoms and F and H atoms can help predict the arrangement of CO_2 molecules around DFE. However, unlike the DFE / CO_2 spectra, this structure does not have literature data from a previous study, which made this study a little more challenging. When identifying the DFE / $(CO_2)_3$ tetramer (Chapter 2), most of its structural arrangements were derived from and compared with the DFE / CO_2 dimer which had been previously studied.[1] No such comparison was possible for the pure DFE cluster.

3.2 Spectral analysis (Experimental)

One chirped-pulse Fourier-transform microwave (CP-FTMW) spectrum of DFE was used here with 1% DFE (in the absence of CO_2). Ne was used as the carrier gas and it was delivered to the chamber at around 30 psig ($\sim 1.6 \times 10^3$ Torr). As there are no variable concentration scans available like observed with the DFE / CO_2 spectra, the intensity variation cannot be observed in pure DFE scan, since the pure DFE species, had only one scan. One spectrum was identified in the pure DFE scan. However that identified pure DFE spectrum can also be identified in all the DFE / CO_2 spectra with an intensity lower than in pure DFE, and hence intensity variations of pure DFE can be studied in DFE / CO_2 scans.

48

For this experiment also, the University of Virginia (UVa) spectrometer (CP-FTMW, chirped-pulse Fourier-transform microwave spectrometer) was used. It provided averages of 400,000 individual spectra within 2 − 8 GHz range.[2] In the scan, the first constant difference pattern (a set of four peaks with the same distance in between 1st and 2nd as well as 3rd and 4th peaks) was found around 5160 MHz (Figure 3.1). As this sample mixture has one spectrum, the information that can be obtained from the Origin application is minimal. Usually, SVIEW is used for quantitative measurements.[3] The intensity of the peaks is related to the net dipole moment of the resultant clusters. The intensity also varies with the number of responsible clusters or molecules present in the experiment.
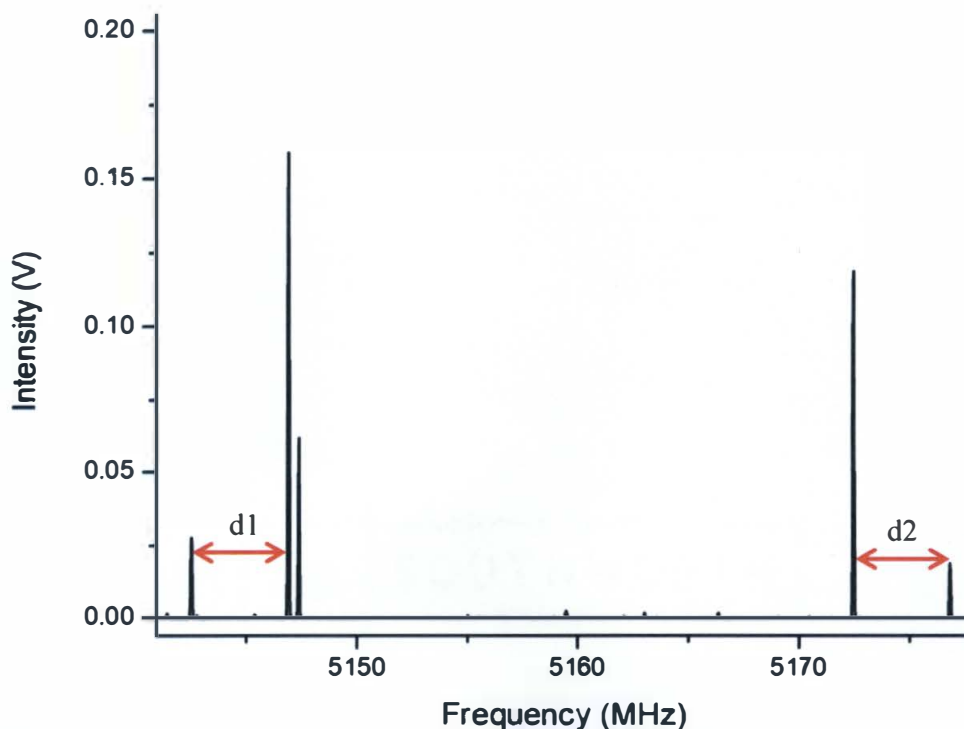
Figure 3.1 - Constant difference pattern in Origin. The uncertainty of d1 and d2 should be less than 4 kHz

Table 3.1 - Frequencies of constant difference patterns

P1 (MHz)	P2 (MHz)	P3 (MHz)	P4 (MHz)	P1 – P2 (d1) (MHz)	P3 – P4 (d2) (MHz)	d1 – d2 (MHz)	Mid point (MHz)
7023.9538	7023.4265	7019.5791	7019.0514	0.5274	0.5277	0.0003	7021.5028
5176.8339	5172.4589	5146.9023	5142.5269	4.3750	4.3755	0.0005	5159.6806
3389.9245	3359.9956	3257.9225	3227.9910	29.9289	29.9315	0.0026	3308.9591

When compared to DFE / CO_2, the DFE only scan is less populated with lines. Three constant difference patterns were found roughly equidistant to one another (Table 3.1). The frequency difference to the midpoint of each neighboring pattern is ~ 1855 MHz and the arrangement of the individual peaks are also very similar, so it is fair to believe that all three constant difference patterns belong to one spectrum. No patterns belonging to this spectrum were found below 3227 MHz or beyond the 7023 MHz as the scan is limited to the range 2 GHz to 8 GHz, but according to the pattern, additional patterns should be observed 1850 MHz below 3308 MHz and 1850 MHz above 7021 MHz. Also, no constant difference patterns were found between these mentioned patterns. That suggests that the three said constant difference patterns belong to adjacent quantum number transitions such as $(n+1) - (n)$, $(n+2) - (n+1)$, and $(n+3) - (n+2)$. After a few trials of setting n to 0, 1, 2,…etc, it was found that those transitions are the 2 - 1, 3 - 2, and 4 - 3 J transitions, so according to this data $J = 1 - 0$ should be observed 1850 MHz below 3308 MHz which is ~ 2A. Then using SPFIT application, the three experimental rotational constants were obtained (Figure 3.2).[3] A total of 77 transitions were assigned with three rotational constants and five distortion constants (Table 3.2).

Parallel to this experimental analysis, the theoretical structure optimization was also done using Gaussian09W at ωB97X-D/6-31+G(d,p) level.[4] This will be more

thoroughly discussed in the structure optimization part (3.3 Theoretical analysis). The structure optimization was done for DFE dimers, DFE trimers, DFE tetramers, and DFE pentamers. It was found that the theoretical rotational constants of the trimer compare well with the experimental rotational constants. All transition frequencies are listed with their theoretical values and quantum numbers in Table 3.3. It can be seen that most Experimental – Calculated frequency differences are less than one kilohertz (1 kHz).

Table 3.2 - Experimental rotational and distortion constants of possible (DFE)₃ trimer structure.

Parameters	Experimental values
A / MHz	930.78807(17)
B / MHz	567.66696(9)
C / MHz	435.66047(8)
Δ_J / kHz	0.4156(8)
Δ_{JK} / kHz	0.374(5)
Δ_K / kHz	0.866(7)
δ_J / kHz	0.1030(3)
δ_K / kHz	0.477(4)
$\Delta v_{rms}{}^a$ / kHz	0.2
N	77

$^a \Delta v_{rms} = \left(\frac{\Sigma(v_{obs} - v_{calc})^2}{N} \right)^{1/2}$; N means the number of transitions in the spectrum.
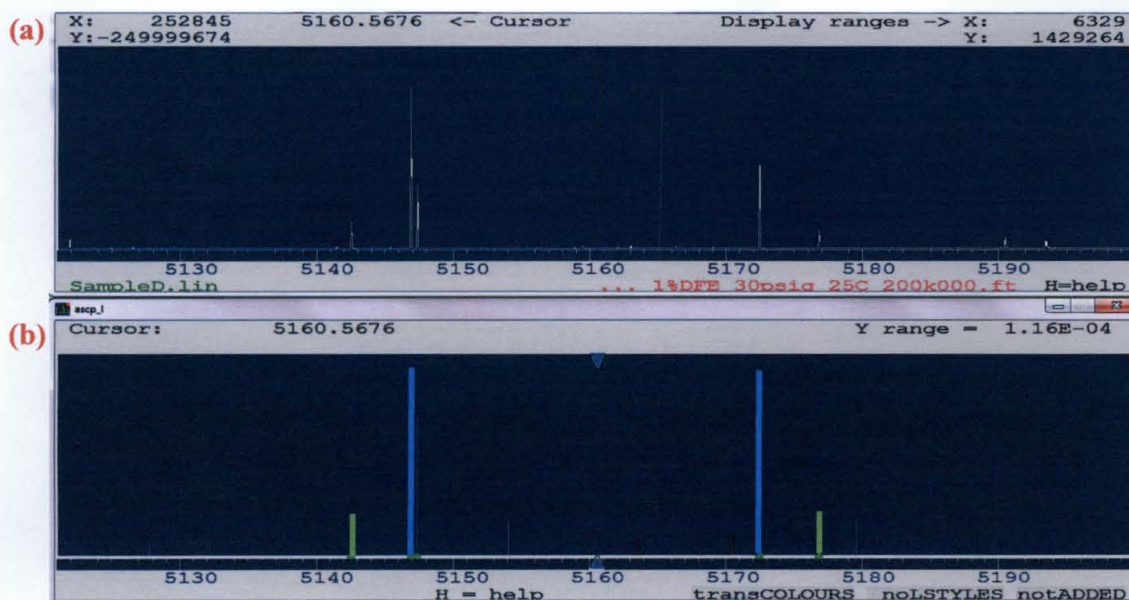
Figure 3.2 - Spectroscopic assignment of (DFE)$_3$ using AABS and SPFIT/SPCAT programs. (a). Experimental rotational spectrum. (b). The predicted spectrum (theoretical). Transitions are (left to right) (J_{KaKc}) : $3_{31} - 2_{20}$, $3_{30} - 2_{20}$, $3_{31} - 2_{21}$, $3_{30} - 2_{21}$

3.3 Computational analysis (Theoretical)

Theoretical analysis of the structure could be done by the two methods discussed in Chapter 2, which are ABCluster method and the manual orientation method. For this DFE study, there are two main disadvantages with manual orientation over ABCluster. The first one, common to DFE / CO$_2$ study as well, is that the guessing of stable arrangements of the structures in three-dimensional space becomes harder when the clusters get bigger. The second problem is, as there are no studies done for DFE structures, as there were for DFE / CO$_2$, there are no literature facts that could be applied to pure DFE cluster spectra. For example, identified DFE / CO$_2$ structures helped to confirm the ABCluster parameters for DFE molecule. Moreover, DFE / CO$_2$ dimer arrangement can be seen in the trimer and tetramer, so dimer literature helped to validate the bigger structures, but no such insight was available for pure DFE. Hence, ABCluster was used from the beginning.

Table 3.3 - Fitted rotational transitions of the identified spectrum

J'	K'_a	K'_c	J''	K''_a	K''_c	Exp. (MHz)	Exp. − Calc. (kHz)
2	1	1	1	0	1	2633.7666	0.7
3	0	3	2	1	2	2638.0967	1.3
2	2	1	1	1	0	3227.9910	-0.5
2	2	0	1	1	0	3257.9225	-0.3
2	2	1	1	1	1	3359.9956	0.4
2	2	0	1	1	1	3389.9245	-2.0
4	0	4	3	1	3	3619.6120	1.0
3	1	2	2	0	2	3843.6229	-1.1
4	1	4	3	0	3	3857.0867	0.9
5	1	4	4	2	2	4094.0917	0.7
3	2	2	2	1	1	4099.2779	-0.7
7	2	6	6	3	4	4238.4949	1.2
3	2	1	2	1	1	4240.0014	-1.1
5	1	4	4	2	3	4471.0239	0.9
3	2	2	2	1	2	4495.2853	0.4
5	0	5	4	1	4	4555.1508	1.4
6	2	4	5	3	2	4670.9153	1.8
5	1	5	4	0	4	4672.8224	2.0
6	1	5	5	2	3	4846.6415	0.0
8	2	7	7	3	5	4861.3794	-0.7
4	2	3	3	1	2	4902.3298	-0.4
8	3	6	7	4	4	5006.8364	-1.0
3	3	1	2	2	0	5142.5269	-0.9
3	3	0	2	2	0	5146.9023	-0.4
4	1	3	3	0	3	5147.3735	0.6
3	3	1	2	2	1	5172.4589	-0.1
3	3	0	2	2	1	5176.8339	-0.1
4	2	2	3	1	2	5279.2618	-0.3
7	1	6	6	2	4	5393.2663	-0.4
9	4	6	8	5	4	5456.1074	-1.1
6	0	6	5	1	5	5458.7662	1.0
6	1	6	5	0	5	5511.6484	2.6
6	1	5	5	2	4	5600.1107	0.8
5	2	4	4	1	3	5649.6584	1.0
4	2	3	3	1	3	5689.9514	-1.6
8	1	7	7	2	5	5766.2507	-0.3
7	2	5	6	3	3	5807.3186	-0.4
9	3	7	8	4	5	5829.2305	-3.8
10	2	9	9	3	7	5870.3944	-2.8
9	4	5	8	5	3	5910.2125	0.4

J'	K_a'	K_c'	J''	K_a''	K_c''	Exp. (MHz)	Exp. – Calc. (kHz)
9	1	8	8	2	6	6031.1273	-1.5
8	3	5	7	4	3	6037.6516	0.7
4	3	2	3	2	1	6083.9709	-0.2
4	3	1	3	2	1	6113.6473	-0.1
4	3	2	3	2	2	6224.6949	-0.1
4	3	1	3	2	2	6254.3719	0.6
10	1	9	9	2	7	6260.9645	-0.4
7	0	7	6	1	6	6344.7377	1.0
7	1	7	6	0	6	6367.0056	2.1
6	2	5	5	1	4	6368.7464	1.5
5	2	3	4	1	3	6403.1260	0.3
10	4	7	9	5	5	6443.7779	-6.8
5	1	4	4	0	4	6541.3647	-0.3
7	1	6	6	2	5	6652.7421	0.1
8	2	6	7	3	4	6764.5650	-2.0
5	2	4	4	1	4	6939.9435	-1.1
5	3	3	4	2	2	6940.1163	-0.3
4	4	1	3	3	0	7019.0514	-0.4
4	4	0	3	3	0	7019.5791	-0.4
4	4	1	3	3	1	7023.4265	-0.3
4	4	0	3	3	1	7023.9538	-0.6
5	3	2	4	2	2	7051.3986	0.8
7	2	6	6	1	5	7097.4955	1.1
8	0	8	7	1	7	7222.1601	0.7
8	1	8	7	0	7	7231.1312	2.4
10	4	6	9	5	4	7282.2383	-2.0
5	3	3	4	2	3	7317.0488	0.2
9	3	6	8	4	4	7338.8923	-1.9
11	4	8	10	5	6	7362.7267	12.7
8	2	6	7	3	5	7392.1493	-0.2
5	3	2	4	2	3	7428.3301	0.3
9	2	7	8	3	5	7491.8910	-4.2
6	2	4	5	1	4	7628.2204	0.1
8	1	7	7	2	6	7632.9280	0.1
6	3	4	5	2	3	7705.6422	-0.1
8	2	7	7	1	6	7864.1732	1.0
6	1	5	5	0	5	7984.9034	-1.6

3.3.1 Dimer optimization

The structural optimization was started with the $(DFE)_2$ dimer. For that, the .xyz files were imported from the DFE / CO_2 tetramer studies. The validity of the parameters used for DFE has been discussed in the previous Chapter 2.5 section. Hence, that .xyz file was used for these DFE structure calculations.

It is worth mentioning the changes in the cluster file when it was used for the DFE only structures (Figure 3.3). The cluster file describes the number of different molecules that need to be used; for example here it is only DFE molecule, so 1. It also describes how many of the molecules are in the structure and for DFE dimer, that is two.

.Cluster file
1 ⟵————————————— **# of different molecules/ .xyz files**
dfe.xyz 2 ⟵————————————— **# of DFE in the cluster**
co2.xyz 3 ⟵————————————— **No CO_2 in the cluster**
* 10.0000

Figure 3.3 - Cluster file for $(DFE)_2$ Dimer

The next file required was .inp file. It identifies the responsible cluster and the number of local minima to be produced. When these files were run, the 0th structure, the structure claimed by ABCluster as the global minimum, is shown in Figure 3.4. Before the rotational constant comparison, it is worth looking at the dipole moments of the 0th structure. From the values of the optimized structure.

$$\mu_A = 0.0000002 \text{ Debye}$$
$$\mu_B = -0.0000001 \text{ Debye}$$
$$\mu_C = -0.0000340 \text{ Debye}$$
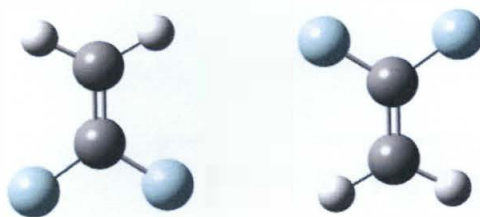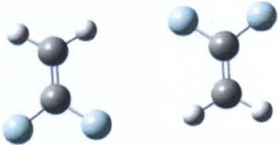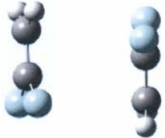
Figure 3.4 - The 0th structure of $(DFE)_2$ dimer

All μ values are very small. Theoretically, this dimer should have zero dipole moment because of the structural arrangement and its symmetry, but the calculated values give very small dipole components because of the errors associated with the calculations. When comparing the experimental rotational constants with these theoretical values, the rotational constant A is far apart from the experimental A value (Table 3.4). The next three lowest energy $(DFE)_2$ dimer structures also have the same discrepancy with A experimental rotational constant, so it is not important to study $(DFE)_2$ dimer further, but $(DFE)_3$ trimer should be studied. The optimized lowest energy structures are mentioned in Table 3.4 to get an idea about the discrepancy in experimental and theoretical rotational constants.

Table 3.4 - Experimental and (DFE)$_2$ theoretical dimer rotational constant comparison

Structure	A (MHz)	B (MHz)	C (MHz)	$\%\Delta B_{avg}$
Experimental	930.78807(17)	567.66696(9)	435.66047(8)	
0th	5208	596	535	228
1st	5213	581	523	227
2nd	2791	1048	1045	153
4th	3506	763	746	159

3.3.2 Trimer optimization

The trimer optimization was done again using ABCluster and optimized by Gaussian09W at ωB97X-D/6-31+G(d,p) level (Table 3.5). Among all these, the 0th structure has a very close comparison with the experimental values while the other structures are not that close to the experimental values. Hence it is believed the structure responsible for the experimental value is a (DFE)$_3$ trimer. To come to that conclusion,

57
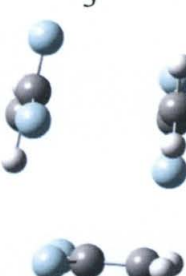
(DFE)$_4$ tetramer and (DFE)$_5$ pentamer were also optimized, but none of them are comparable with the experimental rotational constant values. Their relative energies were also studied (Table 3.5) to find the most stable structure. The 1st and the 4th structure obtained from ABCluster were found to have energies even higher than the 6th structure when those were optimized. Hence those structures do not appear in Table 3.7, where it compares stable theoretical structures with the experimental values.

3.3.3 Tetramer and other structural optimization

The theoretical dimer constants have higher rotational constant values than the experimental constants. The trimer rotational constants are around the experimental values, and the DFE tetramer values are expected to be lower than the experimental values and pentamer values are even smaller than tetramer. However, to complete the structure optimization, the tetramer and pentamer were also optimized (Table 3.6).

Comparing the experimental rotational constant with the optimized theoretical rotational constants, it can be concluded that the most comparable values are for the trimer 0th structure. The values of all the 0th structures can be summarized (Table 3.7).

Table 3.5 - Experimental and (DFE)$_3$ theoretical trimer rotational constant comparison

Structure	A (MHz)	B (MHz)	C (MHz)	$\%\Delta B_{avg}$	Relative energy (Energy − Min. Energy) ($J\,mol^{-1}$)
Experimental	930.78807(17)	567.66696(9)	435.66047(8)		
0th	890	567	420	2.9	76.96
1st	728	575	378	13.1	1594.41
2nd	896	556	415	3.5	73.03
3rd	894	556	415	3.6	134.61

59
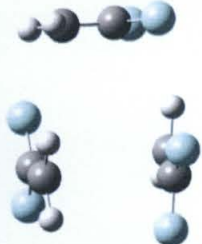
Structure	A (MHz)	B (MHz)	C (MHz)	$\%\Delta B_{avg}$	Relative energy (Energy – Min. Energy) ($J\,mol^{-1}$)
4th	719	565	368	14.6	1562.73
6th (The lowest energy)	892	560	416	3.5	0.00

Table 3.6 - Experimental rotational constant comparison with the 0th structures of tetramer and pentamer

Structure	A (MHz)	B (MHz)	C (MHz)	$\%\Delta B_{avg}$
Experimental	930.78807(17)	567.66696(9)	435.66047(8)	
Tetramer – (DFE)$_4$	349	345	304	48.3
Pentamer – (DFE)$_5$	256	223	184	65.7

Table 3.7 - A comparison of the experimental rotational constants with the rotational constants of dimer, trimer, tetramer, and pentamer

Parameters	Experimental values	Dimer 0th $(DFE)_2$	Trimer 0th $(DFE)_3$	Trimer 6th $(DFE)_3$	Tetramer 0th $(DFE)_4$	Pentamer 0th $(DFE)_5$
A / MHz	930.78807(17)	5208	890	892	349	256
B / MHz	567.66696(9)	596	567	560	345	223
C / MHz	435.66047(8)	535	420	416	304	184
μ_a / D	weakest	0.0	0.4	0.4	0.0	0.2
μ_b / D	weak	0.0	1.0	1.0	0.0	1.4
μ_c / D	strong	0.0	0.5	0.5	0.2	0.5
P_{aa} / u Å^{2} [a]	753.6721(5)	847.3	763.0	775.4	838.4	1514.8
P_{bb} / u Å^{2} [a]	406.3568(5)	97.0	439.3	439.1	822.1	1225.6
P_{cc} / u Å^{2} [a]	136.6016(5)	0.0	128.4	127.8	624.8	747.5
$\%\Delta B_{avg}$ [b]		227.8	2.9	3.5	48.3	65.7
Δv_{rms} [c] /kHz	0.2					
N	77					

[a] Planar moment $P_{aa} = 0.5(I_b + I_c + I_a) = \sum_i m_i r_i^2$

[b] Percent difference between experimental and calculated rotational constants of each sized cluster. ($B_x = A, B, C$) ($\%\Delta B_x = (\sum(B_x(obs)-B_x(calc)/B_x(obs))\times100\%$).

[c] $\Delta v_{rms} = \left(\frac{\sum(v_{obs}-v_{calc})^2}{N}\right)^{1/2}$

In conclusion, $(DFE)_3$ trimer is responsible for the experimental spectrum. Using ABCluster $(DFE)_3$ trimer structures were guessed and using Gaussian09W those $(DFE)_3$ structures were optimized at ωB97X-D/6-31+G(d,p) level. Out of all the structures obtained from ABCluster and then optimized, $(DFE)_3$ 6th structure has the lowest energy

structure followed by $(DFE)_3$ 0th structure (Table 3.5). The structural difference between 0th structure and 6th structure of $(DFE)_3$ trimer is very small which would show little difference between the calculations. Also when compared with P_{aa}, P_{bb}, and P_{cc} values, both structures are very similar to the experimental values. Additionally, this experimental spectrum was observed in DFE/CO_2 scans as well. When considering the $\%\Delta B_{avg}$, the values are closer to 0th structure than the 6th structure, so after considering the rotational constants and the relative energy comparison, the best fitting structure with the experimental rotational constants is the 0th structure (Figure 3.7).
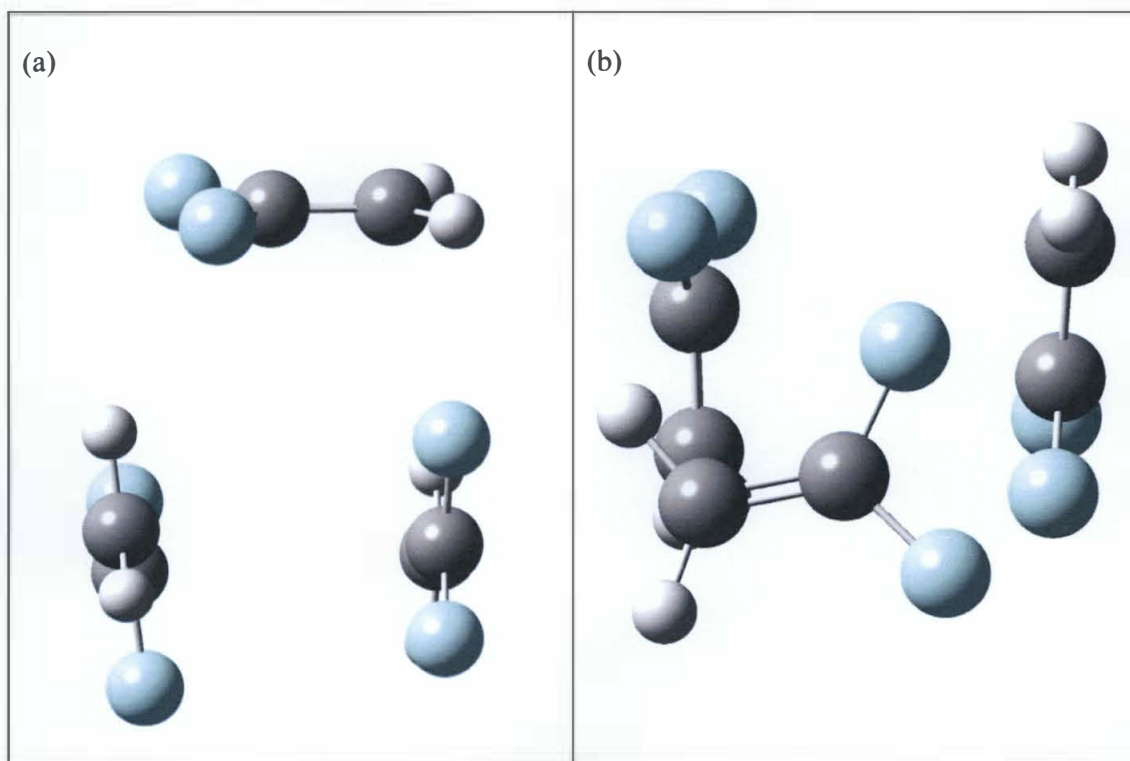

Figure 3.5 – (a) The most comparable theoretical $(DFE)_3$ trimer structure. (b) The top view of the theoretical $(DFE)_3$ trimer structure

References

[1] Anderton, A. M.; Peebles, R. A.; Peebles, S. A. Rotational Spectrum and Structure of the 1,1-Difluoroethylene···Carbon Dioxide Complex. *J. Phys. Chem. A*. **2016**, *120*, 247.

[2] Brown, G. G.; Dian, B. C.; Douglass, K. O.; Geyer, S. M.; Shipman, S. T.; Pate, B. H. A broadband Fourier transform microwave spectrometer based on chirped pulse excitation. *Rev. Sci. Instrum.* **2008**, *79*, 053103.

[3] Kisiel, Z.; Pszczolkowski, L.; Medvedev, I. R.; Winnewisser, M.; De Lucia, F. C.; Herbst, E. Rotational Spectrum of Trans-Trans Diethyl Ether in the Ground and Three Excited Vibrational States. *J. Mol. Spectrosc.* **2005**, *233*, 231.

[4] Frisch, M. J.; Trucks, G. W.; Schlegel, H. B.; Scuseria, G. E.; Robb, M. A. Cheeseman, J. R.; Scalmani, G.; Barone, V.; Mennucci, B.; Petersson, G. A.; Nakatsuji, H.; Caricato, M.; Li, X.; Hratchian, H. P.; Izmaylov, A. F.; Bloino, J.; Zheng, G.; Sonnenberg, J. L.; Hada, M.; Ehara, M.; Toyota, K.; Fukuda, R.; Hasegawa, J.; Ishida, M.; Nakajima, T.; Honda, Y.; Kitao, O.; Nakai, H.; Vreven, T.; Montgomery, Jr., J. A.; Peralta, J. E.; Ogliaro, F.; Bearpark, M.; Heyd, J. J.; Brothers, E.; Kudin, K. N.; Staroverov, V. N.; Keith, T.; Kobayashi, R.; Normand, J.; Raghavachari, K.; Rendell, A.; Burant, J. C.; Iyengar, S. S.; Tomasi, J.; Cossi, M.; Rega, N.; Millam, J. M.; Klene, M.; Knox, J. E.; Cross, J. B.; Bakken, V.; Adamo, C.; Jaramillo, J.; Gomperts, R.; Stratmann, R. E.; Yazyev, O.; Austin, A. J.; Cammi, R.; Pomelli, C.; Ochterski, J. W.; Martin, R. L.; Morokuma, K.; Zakrzewski, V. G.; Voth, G. A.; Salvador, P.; Dannenberg, J. J.; Dapprich, S.; Daniels, A. D.; Farkas, O.; Foresman, J. B.; Ortiz, J. V.; Cioslowski, J.; Fox, D. J. Gaussian 09, Revision E.01, Gaussian, Inc., Wallingford CT, **2013**.

Chapter 4

4. Discussion and Conclusion

4.1 Spectroscopic constants and structural comparison

4.1.1 DFE / CO_2 studies

After configuring the composition of the cluster as DFE / $(CO_2)_3$, the structural arrangement was considered. Using the manual method, 20 different structures were optimized, while using ABCluster 40 different structures were identified, and the theoretical lowest energy structure of DFE / $(CO_2)_3$ was obtained using *ab initio* calculations in Gaussian09W at ωB97X-D/6-31+G(d,p) level.[1] The observed lowest energy structure (0th structure from ABCluster), can be seen from Figure 4.1 (a) and (b). It appears that all 3 CO_2 molecules prefer to be located above the DFE plane and all on one side of DFE.
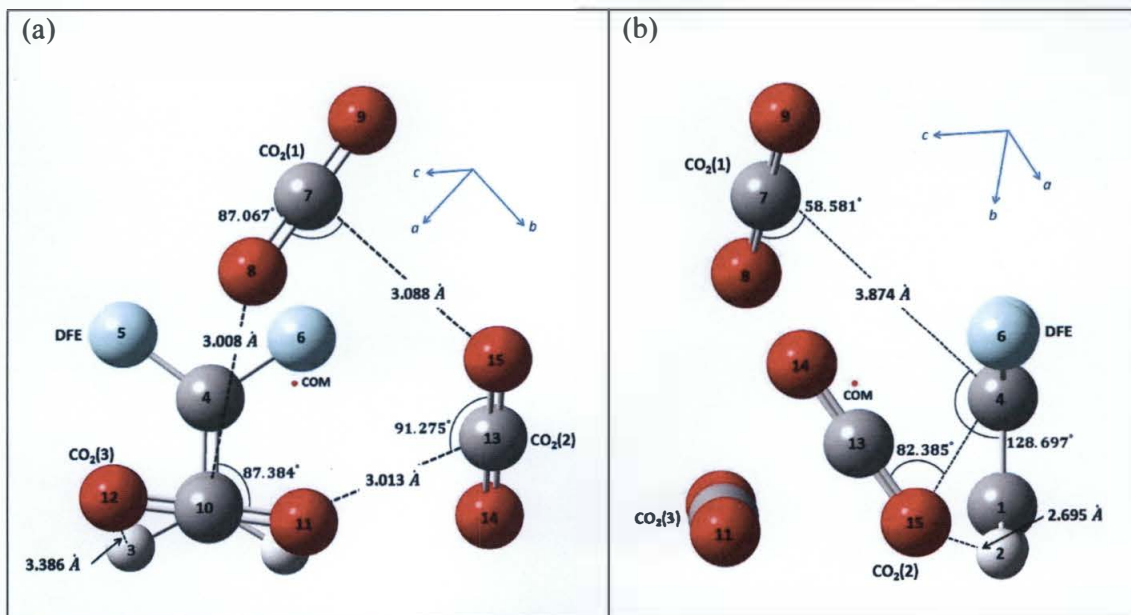

Figure 4.1 - (a) The most comparable DFE / $(CO_2)_3$ tetramer structure with the experimental spectroscopic constants (b) The side-view of the structure. COM stands for the place where the center of mass is located. The optimization was done in Gaussian09W at ωB97X-D/6-31+G(d,p) level

In this study, the goal was to identify the experimental rotational constants and to optimize the structures to match the experimental rotational constants. So far, one spectrum was found experimentally which results in the experimental rotational constants. Then the theoretical structures were optimized to attempt to match the experimental rotational constants (Table 4.1). For 113 assigned peaks, five distortion constants were used.

The five distortion constants used brought Δv_{rms} to 2.3 kHz. The maximum uncertainty allowed here is 4.0 kHz. So for 113 lines, this Δv_{rms} is a good and acceptable value. None of the P_{aa}, P_{bb} and P_{cc} are close to zero, and P_{aa} and P_{bb} are higher than P_{cc} which means the masses are spread along the a and b axes more than along the c axis. Also, the planar moments can be justified from the structural arrangement (Figure 4.1). All the CO_2 molecules are placed on one side of the DFE plane, and the c axis is almost perpendicular to the DFE plane. All the molecules are located roughly parallel to the plane of DFE, except $CO_2(2)$. The ab plane is placed in between CO_2 and DFE molecules roughly parallel to DFE and $CO_2(1)$ and $CO_2(3)$. Also it can be observed that the a axis moves very close to (5) and (6) fluorine atoms, the heaviest atom in this structure, with the CO_2 molecules spread along it. Similarly, for P_{bb}, the b axis runs between the triangle of CO_2 molecules, meaning mass is distributed along the axis, so P_{aa} and P_{bb} have higher values.

The spectroscopic assignment was done using Kisiel's AABS program.[2] The peak assignment was started with transitions having the lowest J values (1, 2, 3), as they appeared with the highest intensity when compared with all transitions responsible for

DFE / $(CO_2)_3$ tetramer. When compared with the DFE / CO_2 dimer, the DFE / $(CO_2)_3$ tetramer has ~ 10% of the dimer intensity.[3]

Table 4.1 - Experimental and theoretical spectroscopic constants of DFE / $(CO_2)_3$ tetramer

Parameters	Experimental values	Tetramer 0th DFE / $(CO_2)_3$
A / MHz	638.36285(11)	634
B / MHz	608.12956(12)	581
C / MHz	548.61474(11)	532
Δ_J / kHz	0.2641(21)	
Δ_{JK} / kHz	0.218(9)	
Δ_K / kHz	0.031(8)	
δ_J / kHz	0.0506(11)	
δ_K / kHz	-0.149(6)	
μ_a / D	strong	0.9
μ_b / D	weak	1.0
μ_c / D	weakest	0.1
$P_{aa}{}^a$ / amu $\mathring{A}^2$	480.2748(5)	511.0
P_{bb} / amu $\mathring{A}^2$	440.9163(5)	439.5
P_{cc} / amu $\mathring{A}^2$	350.7636(5)	358.1
$\%\Delta B_{avg}{}^b$		2.7
$\Delta v_{rms}{}^c$ / kHz	2.3	
# of peaks	113	

[a] Planar moment $P_{aa} = 0.5(I_b + I_c + I_a) = \sum_i m_i r_i^2$

[b] Percent difference between experimental and calculated rotational constants of each sized cluster. ($B_x = A, B, C$) ($\%\Delta B_x = (\Sigma(B_x(\text{obs})-B_x(\text{calc})/B_x(\text{obs}))\times100\%$).

[c] $\Delta v_{rms} = \left(\frac{\Sigma(v_{obs}-v_{calc})^2}{N}\right)^{1/2}$

4.1.2 Pure DFE studies

The optimization was done using Gaussian09W at ωB97X-D/6-31+G(d,p) level.[1] The outputs obtained from ABCluster were taken as the input files for this optimization. $(DFE)_2$ dimer, $(DFE)_3$ trimer, $(DFE)_4$ tetramer, and $(DFE)_5$ pentamer structures were optimized and compared with the experimental rotational constants. The most comparable values were found with the trimer structures (Table 4.2). Among more than 40 optimized structures, the 0th energy of the trimer structure gave the best comparison with the experimental spectroscopic constants. In this structure (Figure 4.2), one F of DFE(2) molecule is facing the DFE(3)'s F atom. This causes the top DFE(2) to show a leftward distortion away from the right side DFE(3) because of fluorine – fluorine repulsion; however, DFE(1) and DFE(3) molecules maintain the 3rd most stable dimer structure's orientation.
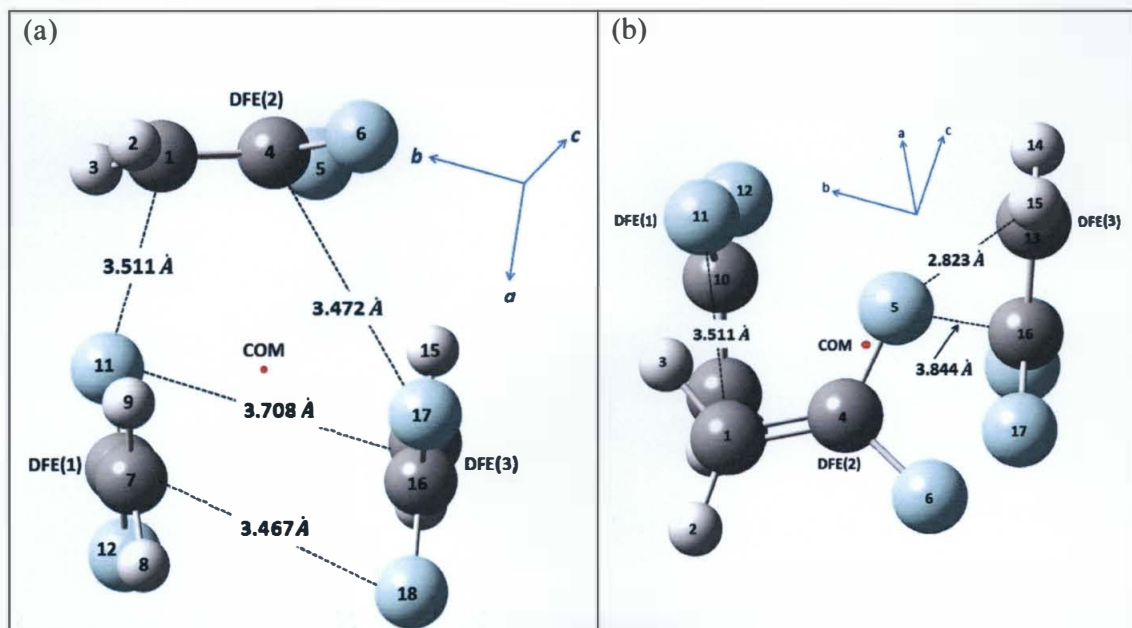

Figure 4.2 – (a). The most comparable $(DFE)_3$ structure with the experimental spectroscopic constants. (b). The top-view of the $(DFE)_3$ trimer structure. COM stands for the place where the center of mass is located. The optimization was done in Gaussian09W at ωB97X-D/6-31+G(d,p) level

Table 4.2 - Experimental and theoretical spectroscopic constants of (DFE)₃ trimer

Parameters	Experimental values	Trimer 0th (DFE)$_3$
A / MHz	930.78807(17)	890
B / MHz	567.66696(9)	567
C / MHz	435.66047(8)	420
Δ_J / kHz	0.4156(8)	
Δ_{JK} / kHz	0.374(5)	
Δ_K / kHz	0.866(7)	
δ_J / kHz	0.1030(3)	
δ_K / kHz	0.477(4)	
μ_a / D	weakest	0.4
μ_b / D	weak	1.0
μ_c / D	strong	0.5
$P_{aa}{}^a$ / amu $\mathring{A}^2$	753.6721(5)	763.0
P_{bb} / amu $\mathring{A}^2$	406.3568(5)	439.3
P_{cc} / amu $\mathring{A}^2$	136.6016(5)	128.4
$\%\Delta B_{avg}{}^b$		-2.9
$\Delta\nu_{rms}{}^c$ / kHz	0.2	
# of peaks	77	

^{a} Planar moment $P_{aa} = 0.5(I_b + I_c + I_a) = \Sigma_i m_i r_i^2$

^{b} Percent difference between experimental and calculated rotational constants of each sized cluster. ($B_x = A, B, C$) ($\%\Delta B_x = (\Sigma(B_x(obs)-B_x(calc)/B_x(obs))\times100\%$).

^{c} $\Delta\nu_{rms} = \left(\frac{\Sigma(\nu_{obs}-\nu_{calc})^2}{N}\right)^{1/2}$

69

4.2 Calculation method

The optimization method, based on density functional theory (DFT), might not be the most accurate optimization method available but was the best to use due to the structure size and the level of optimization required. However, for the 0th structure of DFE / $(CO_2)_3$ the calculation was again run with MP2/6-311++G(2d,2p) format for comparison. According to the results and the optimization time, the utilization of the DFT optimization method can be justified, because as shown in Table 4.3, the DFT optimization took only around one and a half hours to optimize the structure. With MP2/6-311++G(2d,2p) format, it took 43 hours and 40 minutes, which is nearly 30-fold the time span taken by DFT method. For one cluster optimization, around 40 different structures were optimized. So it is not convenient to use that MP2 format to study these structures at this initial level with the facilities available. The optimization calculations were solely done in a Core-i5 computer with a 3.4 GHz processor and 4.0 GB of RAM. The performance of the computer has an impact on the optimization time.

In Table 4.3 there is a discrepancy seen in the dipole moment section. The relative intensities of theoretical dipole moments do not agree with the experimental dipole moment (qualitatively estimated using line intensity) even though the rotational constants are matching. The second strongest experimental dipole moment component (μ_b) does not agree with the theoretical dipole moment, which shows the highest dipole moment component value. Earlier it was suspected this might occur because of the error associated with DFT level calculations. Comparatively, electronic charge distribution is less well described by the DFT method. But the MP2 level and DFT level both show almost the same values and do not agree with the experimental values. This might be

because a small structural change could exist, which could make a larger impact on the overall dipole moment of the structure.

Table 4.3 - Theoretical value comparison in ωB97X-D/6-31+G(d,p) and MP2/6-311++G(2d,2p) formats with the experimental data to understand the cost of optimization and to identify the most convenient optimization format

Parameters of DFE / $(CO_2)_3$	Experimental values	0th structure ωB97X-D/6-31+G(d,p)	0th structure MP2/6-311++G(2d,2p)
A / MHz	638.36285(11)	634	701
B / MHz	608.12956(12)	581	597
C / MHz	548.61474(11)	532	524
μ_a / D	strong	0.9	0.9
μ_b / D	weak	1.0	1.1
μ_c / D	weakest	0.1	0.2
P_{aa} / amu $\dot{A}^2$	480.2748(5)	511.0	545.2
P_{bb} / amu $\dot{A}^2$	440.9163(5)	439.5	419.1
P_{cc} / amu $\dot{A}^2$	350.7636(5)	358.1	301.7
$\%\Delta B_{avg}$		2.7	1.5
Optimization time (CPU time)		1.36 hrs	43.42 hrs

The MP2 calculation method provides better and more accurate theoretical structures as it uses complex but fewer approximations while DFT uses less complex and more approximations. But for this optimization, when the time consumed for optimization is compared, the DFT calculation method is much more time efficient. If the experimental rotational constant values were taken as the exact values, the average percent error allocated with the DFT method is 2.7% but with MP2 method, the average

percent error is 1.5%. However, $\%\Delta B_{avg}$ is considered here and when comparing the average of B with root mean square values (rms), $\%\Delta B_{avg}$ values seems to be misleading as it considers the sign of the difference (so the difference of opposite sign balance each other and cancel) but rms calculations only consider the magnitude of the differences.

The $CO_2(2)$ in Figure 4.3(d) has moved backward more towards the DFE plane, so that it is almost coplanar with the DFE's plane, in the MP2 calculations. The $CO_2(3)$ molecule aligned above the DFE in (a) has moved inclined to DFE's C=C axis (Figure 4.3 (c)). However, from the previous calculations in Chapter 2, it was found that when all the parameters are correct, $CO_2(2)$ prefers to be on the plane of DFE but not perpendicular to DFE. In MP2 optimized structure, $CO_2(3)$ molecule to DFE in Figure 4.3 (d) has similarities with the (III) dimer orientation (Figure 4.4). But when compared with $CO_2(1)$ structure in Figure 4.3, such an arrangement was not identified experimentally in the DFE / CO_2 dimer studies. The structure optimized from DFT method has some similarities with DFE / CO_2 dimer. For Example, DFE and $CO_2(1)$ give a similar structure to DFE / CO_2 dimer (IV) structure. $CO_2(1)$ and $CO_2(3)$ both are roughly located on two planes parallel to the DFE plane. But $CO_2(2)$ is inclined to the DFE plane. If considering the structure which is optimized at MP2 level (Figure 4.3 (c) and (d)), it has more similarities with the DFE / CO_2 dimer structures. $CO_2(2)$ is almost coplanar with DFE and maintains distances similar to DFE / CO_2 dimer structure (I). $CO_2(3)$ and DFE are arranged like the dimer structure (III). So the tetramer structure optimized from MP2 method has more similarities with the dimer structures.
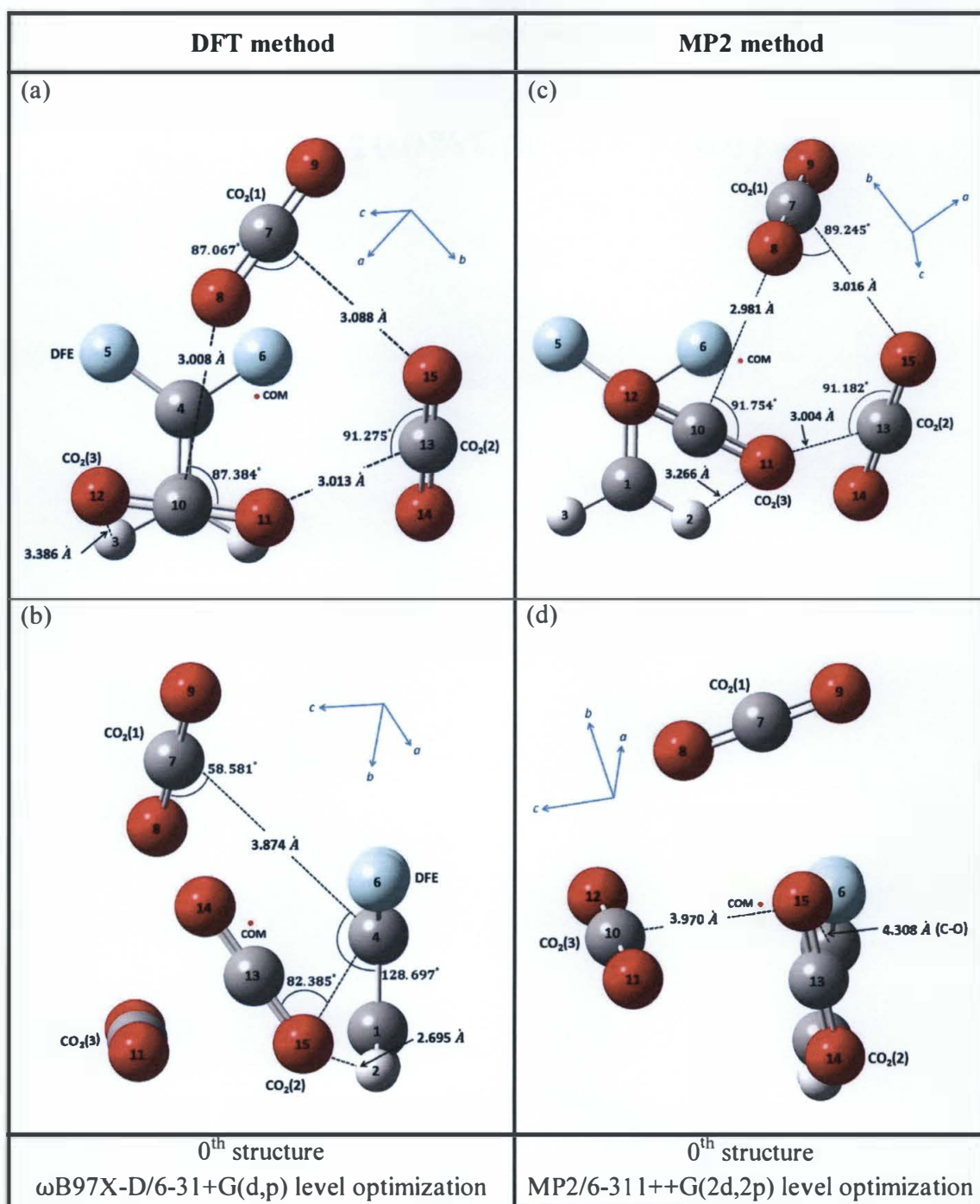
Figure 4.3 – DFE / $(CO_2)_3$ tetramer structure comparison of ωB97X-D/6-31+G(d,p) vs. MP2/6-311++G(2d,2p) level optimization. (a) DFE / $(CO_2)_3$ tetramer optimized in ωB97X-D/6-31+G(d,p) format. (b) Side-view of (a). (c) DFE / $(CO_2)_3$ tetramer optimized in MP2/6-311++G(2d,2p) format. (d). Side-view of (c)
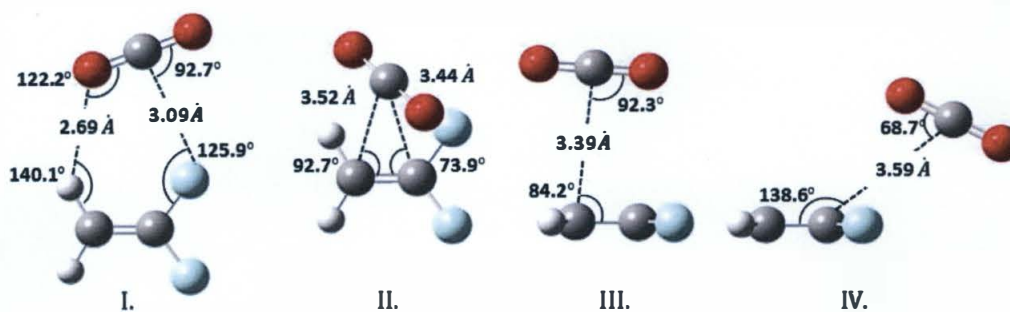
Figure 4.4 - Four most stable structures of DFE⋯CO_2 after zero point energy (ZPE) and basis set superposition error (BSSE) corrections[3]

Usually, moderate-strong hydrogen bonds should have a 1.5 − 2.2 Å intermolecular bond distance and the bond angle should be close to ~ 180°.[4] In reality, weak hydrogen bonds can be observed with bond lengths greater than 2.2 Å, but none of the H atoms show such an arrangement in the DFE / $(CO_2)_3$ tetramer structures. Likewise, the bond angle should be 120° − 180° to make a hydrogen bond but no bond is making such an angle. But in all the structures, the trend seen is that the CO_2(1), (2) and (3) tends to shift towards the 2F of the DFE and move away from 2H. Also, no CO_2 molecule lies on the DFE plane in the DFT level calculation, although in the MP2 calculation it does.

However, in both DFT and MP2 method, three CO_2 tries to maintain the distance between C atom and the nearest neighboring O atom, which is equal to ~ 3.0 Å (Figure 4.3). Also the three CO_2 molecules try to maintain the angle which they make with C-O and the nearest neighbouring O atom, which is roughly equal to 88°.

4.3 $(CO_2)_3$ trimer optimization

In the meantime, the lowest energy structure for $(CO_2)_3$ trimer was deduced using ABCluster and it was optimized with the ωB97X-D/6-31+G(d,p) level in Gaussian09W to find similarities of CO_2 trimer and the three CO_2 in the DFE / $(CO_2)_3$ tetramer (Figure

4.5). The $(CO_2)_3$ trimer has given a pinwheel-like planar structure which tries to maintain ~88° among O-C bond with the nearest neighboring O atom, and the bond lengths between C and the closest neighboring O atom is ~3.0 Å. This can be observed in the DFE / $(CO_2)_3$ tetramer as well. Especially this $(CO_2)_3$ trimer pinwheel structure can be prominently seen in the tetramer, which was optimized in DFT method.
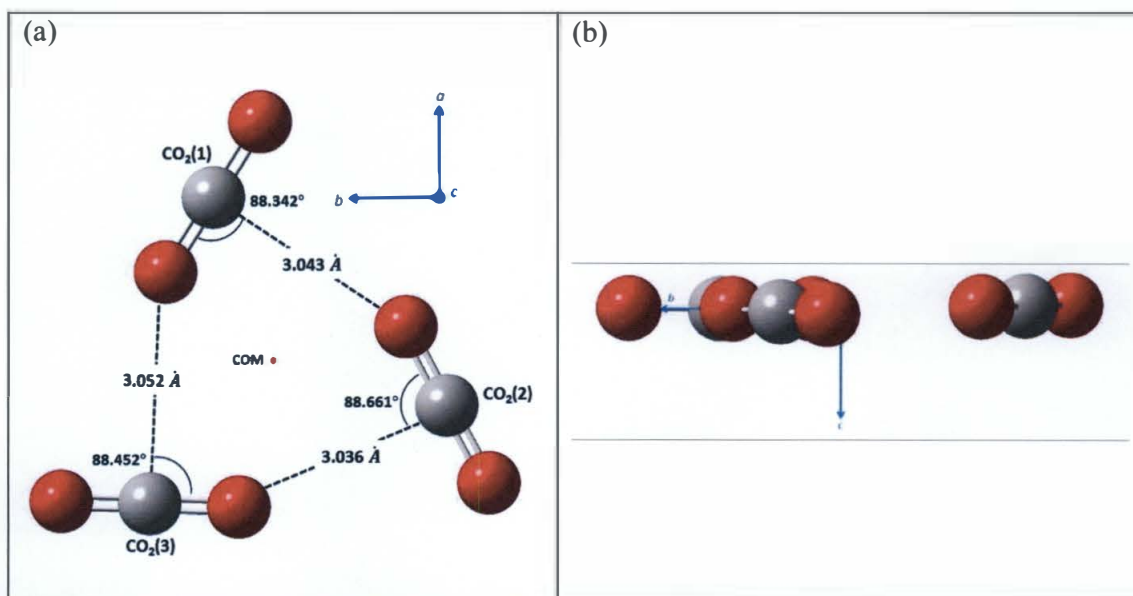
Figure 4.5 - (a) The lowest energy $(CO_2)_3$ trimer obtained from ABCluster and the optimization was done in Gaussian09W at ωB97X-D/6-31+G(d,p) level. (b) The side-view of the $(CO_2)_3$ trimer structure. COM stands for the place where the center of mass is located

This pinwheel structure is not parallel to the DFE plane, but inclined. If one imagines the same plane in which all three carbon atoms of CO_2 lie, the pinwheel can be seen. It maintains almost the same distances and roughly the same angle which is close to 88°. This is evidence to conclude that $(CO_2)_3$ trimer makes a stable cluster, which is strong enough to make the same trimer independently despite the attraction from the DFE molecule.

4.4 Binding energies

When the CO_2 molecule and the DFE molecule were optimized at ωB97X-D/6-31+G(d,p) level in Gaussian09W separately, the energy of the single molecules could be found. So by adding 1 DFE + 3 × CO_2 energies, the energy of the four molecule tetramer can be estimated. When the actual tetramer energy was subtracted from the four molecules energy, the binding energy of the cluster could be found (Table 4.4 and Equation 4.1), and the intermolecular bond strengths and types can be predicted from the observed bond lengths and bond angles. It is hard to find the bond energies of the individual bonds, but it is still important to obtain the bond energy of the cluster to discuss the sc-CO_2 microsolvation.

Table 4.4 - Binding energy calculation for DFE / $(CO_2)_3$ tetramer and the energies of individual molecules to identify the net binding energy of the DFE / $(CO_2)_3$ structure

Structure	Energy (E_h)
DFE	-276.998907320
CO_2	-188.526944623
1 DFE + 3 × CO_2	-842.579741189
DFE / $(CO_2)_3$ tetramer	-842.589848917
Binding energy	-0.0101 (27 kJ/mol)
$(CO_2)_5$ binding energy	-0.0155 (41 kJ/mol)[5]

$$E(DEF...(CO_2)_3) - 3E(CO_2) - E(DEF) = -842.589 - (-276.999 - 3 \times 188.527) = -0.010E_h \quad (4.1)$$

For calculation of the binding energy of the DFE / $(CO_2)_3$ tetramer, the difference of the DFE / $(CO_2)_3$ cluster to the individual energies of the molecules was considered (Table 4.4). It was found that the total binding energy of the DFE / $(CO_2)_3$ tetramer is

equal to 27 kJ/mol (Equation 4.1). When compared with non-covalent intermolecular forces, this value is a small value. For example, for a hydrogen bond the energy is varying between 20 – 30 kJ/mol. But that is for one bond. Even though it is not known the number of bonds that exist in this tetramer, it is obvious that the tetramer cluster makes than one intermolecular bond. Hence the binding energies are smaller. Moazzen-Ahmadi *et al,* have observed the binding energy of $(CO_2)_5$ is equal to 41 kJ/mol.[5] If it is believed that the binding energy is roughly equal on each CO_2 molecule, one CO_2 molecule is responsible for roughly 8 kJ/mol. So that is applicable to this study as well. For example, there are three CO_2 molecules in this tetramer. So it should have 24 kJ/mol. But the entire DFE / $(CO_2)_3$ tetramer has only 27 kJ/mol. Maybe this happens because of the attraction of the DFE molecule; it also can be seen that three CO_2 molecules have been distorted from their pinwheel structure in the tetramer, so it could be believed that CO_2 binding energy is somewhat lesser than the 8 kJ/mol.

Table 4.5 - Binding energy calculation for (DFE)₃ trimer and the energy of individual DFE molecule to identify the net binding energy of the (DFE)₃ structure

Structure	Energy (E_h)
DFE	-276.998907320
(DFE)₃ trimer	-831.003953976
3 × DFE	-830.996721960
Binding energy	-0.0072 (19 kJ/mol)

Likewise, for optimized (DFE)₃ trimer structure, the energy of the cluster was calculated. Then the energy of 1 DFE was calculated. Then the energy of (DFE)₃ trimer was subtracted from three times of 1 DFE energy (Table 4.5 and Equation 4.2), so the total binding energy of the (DFE)₃ is 19 kJ/mol. When compared with the intermolecular

bond energies, this is not a big value. This value is roughly 2/3 of the binding energy of the tetramer.

$$E(\text{DEE})_3 - 3E(\text{DEF}) = -831.003 - (-3 \times 276.999) = -0.007E_h \qquad (4.2)$$

4.5 Comparison of this study with other CO_2 studies

The DFE / $(CO_2)_3$ tetramer has orientations of DFE / CO_2 dimer observable within its structure. It can be seen that the DFE and CO_2 tetramer tries to maintain DFE-CO_2 distances in the dimer even though the number of CO_2 molecules is increased. For example, coplanar DFE-CO_2 can be observed in the DFE / CO_2 tetramer in the MP2 calculations. For structure (I) of DFE / CO_2 dimer study, the C-H---O=C intermolecular bond distance of the dimer is 2.69 $\mathring{A}$ and C-F---C=O intermolecular bond distance is 3.09 $\mathring{A}$. This compares well to the DFE / $(CO_2)_3$ tetramer in MP2 calculations, where the in-plane DFE and CO_2 have a C-H---O=C intermolecular bond distance equal to 2.60 $\mathring{A}$, and C-F---C=O intermolecular bond distance equal to 2.97 $\mathring{A}$. Also, DFE / $(CO_2)_3$ tetramer has all the CO_2 molecules on one side from the DFE plane.

When compared with the VF / CO_2 studies, the number of patterns identified in the DFE / CO_2 scans is fewer.[6] In a VF molecule, there is no symmetry at all. Since VF has only one F, VF has a more different environment to accommodate many CO_2 molecules around a VF molecule, but 1,1-difluoroethene has only one in-plane position to place a CO_2 molecule and so it has a less different environment to accommodate many CO_2 molecules around it. Another goal is to collectively understand with VF and DFE studies, how many CO_2 molecules are required to make the microsolvation shell around DFE and VF.

4.6 Future goals

In the future, this project needs to analyze for the DFE / $(CO_2)_2$ trimer. MathCAD plotting has been started to identify the transitions that behave similarly as the concentration of CO_2 is varied. Such graphs are being used for both the VF / CO_2 studies, preliminary work on DFE / CO_2 studies, and has shown that the DFE / $(CO_2)_3$ tetramer grouped into a cluster on the graph. At this level, more MathCAD calculations are important to identify more patterns, since the transition patterns are largely spaced and hard to observe in the spectrum itself which cannot be easily identified. The DFE / $(CO_2)_2$ trimer was very recently identified by this MathCAD approach, and further analysis is underway.

Apart from that, ^{13}C isotopic studies are needed to confirm the structural results of existing work. The DFE / CO_2 dimer paper has ^{13}C isotopic information and hence the future studies can be compared with the existing information.[1] When isotopic atoms are used, the mass of the molecules change. If ^{13}C is used, the mass will increase, hence the moment of inertia will increase (I) without changing the intermolecular distances. As (I) has an inversely proportional relationship with rotational constants, rotational constants decrease. Also those isotopic values again can be compared with ^{13}C isotopic DFE / CO_2 dimer information and as well as the existing DFE / $(CO_2)_3$ tetramer and $(DFE)_3$ trimer clusters to further confirm the mass distribution in those clusters.

References

[1] Frisch, M. J.; Trucks, G. W.; Schlegel, H. B.; Scuseria, G. E.; Robb, M. A. Cheeseman, J. R.; Scalmani, G.; Barone, V.; Mennucci, B.; Petersson, G. A.; Nakatsuji, H.; Caricato, M.; Li, X.; Hratchian, H. P.; Izmaylov, A. F.; Bloino, J.; Zheng, G.; Sonnenberg, J. L.; Hada, M.; Ehara, M.; Toyota, K.; Fukuda, R.; Hasegawa, J.; Ishida, M.; Nakajima, T.; Honda, Y.; Kitao, O.; Nakai, H.; Vreven, T.; Montgomery, Jr., J. A.; Peralta, J. E.; Ogliaro, F.; Bearpark, M.; Heyd, J. J.; Brothers, E.; Kudin, K. N.; Staroverov, V. N.; Keith, T.; Kobayashi, R.; Normand, J.; Raghavachari, K.; Rendell, A.; Burant, J. C.; Iyengar, S. S.; Tomasi, J.; Cossi, M.; Rega, N.; Millam, J. M.; Klene, M.; Knox, J. E.; Cross, J. B.; Bakken, V.; Adamo, C.; Jaramillo, J.; Gomperts, R.; Stratmann, R. E.; Yazyev, O.; Austin, A. J.; Cammi, R.; Pomelli, C.; Ochterski, J. W.; Martin, R. L.; Morokuma, K.; Zakrzewski, V. G.; Voth, G. A.; Salvador, P.; Dannenberg, J. J.; Dapprich, S.; Daniels, A. D.; Farkas, O.; Foresman, J. B.; Ortiz, J. V.; Cioslowski, J.; Fox, D. J. Gaussian 09W, Revision E.01, Gaussian, Inc., Wallingford CT, **2013**.

[2] Kisiel, Z.; Pszczolkowski, L.; Medvedev, I. R.; Winnewisser, M.; De Lucia, F. C.; Herbst, E. Rotational Spectrum of Trans-Trans Diethyl Ether in the Ground and Three Excited Vibrational States, *J. Mol. Spectrosc.* **2005**, *233*, 231.

[3] Anderton, A. M.; Peebles, R. A.; Peebles, S. A. Rotational Spectrum and Structure of the 1,1-Difluoroethylene···Carbon Dioxide Complex. *J. Phys. Chem. A* **2016**, *120*, 247.

[4] Atkins, P.; Paula, J. D.; Physical Chemistry. 09th edition. **2010**, 637.

[5] Oliaee, N. J.; Dehghany, M.; McKellar, A. R. W.; Moazzen-Ahmadi, N. High resolution infrared spectroscopy of carbon dioxide clusters up to $(CO_2)_{13}$. *J. Chem. Phys.* **2011**, *135*, 044315.

[6] Kannangara, P. B.; West, C. T.; Peebles, S. A.; Peebles, R. A. Towards microsolvation of fluorocarbons by CO_2: Two isomers of fluoroethylene-$(CO_2)_2$ observed using chirped-pulse Fourier-transform microwave spectroscopy. *Chem. Phys. Lett.* **2018**, *706*, 538.